THE EFFECT OF COLD GALVANIZING ZINC COATING AS A CATHODIC PROTECTION ON CORROSION RATE AND BOND STRENGTH OF REINFORCED CONCRETE

By

HYMAN JAFAR JAAF

Bachelor of Engineering – Chemical engineering

University of Technology

Baghdad, Iraq

1993

Submitted to the Faculty of the
Graduate College of the
Oklahoma State University
in partial fulfillment of
the requirements for
the Degree of
MASTER OF SCIENCE
December, 2012

THE EFFECT OF COLD GALVANIZING ZINC COATING AS A CATHODIC PROTECTION ON CORROSION RATE AND BOND STRENGTH OF REINFORCED CONCRETE

Thesis Approved:

Dr. Jim Smay

Thesis Adviser

Dr. Josh Ramsey

Dr. Tyler Ley

Name: HYMAN JAFAR JAAF

Date of Degree: DECEMBER, 2012

Title of Study: THE EFFECT OF COLD GALVANIZING ZINC COATING AS A CATHODIC PROTECTION ON CORROSION RATE AND BOND STRENGTH OF REINFORCED CONCRETE

Major Field: CHEMICAL ENGINEERING

ABSTRACT:

This study focuses on the corrosion rate of steel in reinforced concrete and its effect on the steel rebar physical properties: Rockwell hardness, Vickers hardness, tensile strength, and yield strength. It was no noticeable effect of the corrosion rate of steel rebar on the physical properties. Tafel test was carried out to analyze the effect of pH and salinity on the corrosion rate of the reinforcement steel. Corrosion rate of reinforced concrete for uncoated and cold galvanized zinc coated steel were investigated at different pH and salinity by using weight loss method. The maximum sheer stress required to pull out the steel samples from the concrete was studied at different pH and salinity solutions by bond strength test. The results showed that at low pH ranges (acidic medium), the corrosion rate of the reinforced concrete was higher than at high pH ranges (alkaline medium), i.e. the corrosion rate is inversely proportional to pH. The corrosion rate of reinforced steel is positively proportional to the salinity until a certain salinity concentration, and then inversely proportional to the salinity due to limited oxygen diffusion. It can be concluded that the corrosion rate of the embedded rebar in reinforced concrete affects its structural performance in two ways, either by reducing its cross-section area or by deteriorating the strength of bonds between the steel and concrete.

TABLE OF CONTENTS

LIST OF TABLES

Table Page

LIST OF FIGURES

Figure Page

CHAPTER I

Introduction

Galvanic corrosion of steel is an electrochemical reaction that combines iron with water and oxygen to form hydrated iron oxides (rust) similar in chemical composition to the original iron. Galvanic corrosion requires three factors to occur: (i) two metals with dissimilar electrode potentials, (ii) an electrolyte for ion transport and (iii) electrical contact between the two metals for electron transport. It results in deterioration of the material and its properties. Galvanic corrosion of rebar is a leading cause of failures in reinforced concrete structures, [1].

Several factors in reinforced concrete structures are known to favor corrosion: poor construction and design quality, poor materials selection, and exposure to a corrosive chemical environment, [1].

In some countries with quickly developing infrastructures, poor quality concrete can be a result of implementation of the structures on the basis of economic considerations. In the Middle East, corrosion problems are increased due to the harsh conditions of a warm marine climate and the salinity of ground water. This has led to a short life expectancy of reinforced concrete structures, [2].

In Iraq, there are two major rivers (Tigris and Euphrates) flowing from northern part to southern part of Iraq which accounts for 98% of the water supply in the country. On their path, they have a lot of bridges and hydraulic structures, which needs to be protected. Corrosion of structures in these bridges not only affects the economical aspect but also the safety issues of people traveling across these bridges.

Corrosion affects people's daily lives which includes some of the following damages: failure of a section of highway, the collapse of electrical towers, and damage to buildings, parking structures, and bridges. These damages result in large amount of repair costs and endanger public safety, [1].

The effect of corrosion is not only a worldwide engineering problem but also an economic problem. Because of this economic cost, many production and manufacturing companies, state and federal highway agencies, and infrastructure developers are pursuing corrosion control methods for reinforced concrete structure. Besides the economic importance of corrosion, corrosion control has gained importance due to human safety and conservation, [1].

Prevention of galvanic corrosion is well-understood and requires eliminating one of the three requirements. However, the dissimilar metals in close electrical contact are a micro-structural feature of plain carbon steel, where pearlite microstructure is common. The only viable options are to prevent the metal from coming into contact with an electrolyte and/or place the metal in contact with a more anodic metal such that the rebar is become the cathode in the electrolytic cell and is protected

In this study, a professional cold galvanizing compound zinc spray coating is used as a cathodic protection method to act as a sacrificial anode and protect the steel rebar. Hot-dipped galvanizing is a common galvanizing technique, but this study is intended to evaluate the spray-on zinc coating for stability under various corrosive environments. In cathodic protection, the electrons flow from the more negative potential (more active metal) to the less negative potential (more noble metal). The more negative potential which is the anode corrodes, whereas the less negative potential which is the cathode gets protected, [3].

There are other four chapters contain as following:

Chapter 2 provides a brief description on galvanic corrosion theoretical background and literature review related to this research. This chapter consists sections that introduce galvanic corrosion definition, galvanic cell, types of corrosion, corrosive environments, pH effect, and salinity effect. Also, it includes other sections introduce the reinforced concrete corrosion and its mechanism, passivation, and carbonation definition, and some information about Iraqi water and corrosion protection methods in addition to economic impact of corrosion.

Chapter 3 describes the experiments that were performed for this study by details which include the materials, equipment, sample preparation and experiments procedure. This study depends on three sets of experiments include investigation of the steel rebar physical properties, the effect of different pH and salt concentration on the corrosion rate of rebar embedded in reinforced concrete, and the bond behavior test between the steel rebar and the concrete element.

Chapter 4 presents the experimental results obtained by using three sets of experiments to investigate the effect of pH and salinity on the corrosion rate of reinforced concrete, the bond behavior between the steel rebar and the concrete element immersed in different pH and salt concentration solutions, and the steel rebar physical properties. First experiment investigates a relation between the corrosion rate vs. different pH and salinity ranges for steel rebar using Tafel test method, and weight loss method for uncoated and cold galvanized zinc coated reinforcement steel rebar. Second experiment tests the bond behavior between the steel rebar and the concrete element to investigate the maximum force and shear stress required to cause failure to these bonds for uncoated and zinc coated steel rebar embedded in concrete element, and the last experiment focuses on the physical properties of the steel rebar represented by Rockwell hardness, Vickers hardness, yield strength, and tensile strength.

Chapter 5 introduces conclusion that can be drawn from the results shown in the previous chapter followed by some recommendations.

1.1 The Objective of the work

The objective of the work in this study is to investigate the following:

i. The effect of pH and salinity on reinforced concrete corrosion rate using Tafel test method, and weight loss method.
ii. The effect of pH and salinity on the bond strength between the steel rebar and concrete.
iii. The effect of corrosion rate on the steel rebar physical properties such as hardness, tensile strength, and yield strength.

iv. The effect of cold galvanizing zinc coating process on reducing the corrosion rate under various salinity concentrations, and pH environment conditions, which surround the reinforced concrete element. And determine the effect of zinc coating on the bond strength under the same environment conditions that above mentioned.

Tafel test is conducted to measure the corrosion rate for steel rebar specimens immersed in solutions of different pH and salinity as a corrosive environment. The corrosion measurements will take the advantage of electrochemical test method in order to figure out the corrosion rate in a short period of time.

Corrosion rate of reinforced concrete experiment is carried out using weight loss method for uncoated and zinc coated steel rebar specimens embedded in cylindrical concrete element samples immersed in solutions of different pH and salinity. The effect of pH and salinity on the corrosion rate will be investigated; also the result will provide a good chance to evaluate the corrosion reduction efficiency of cold galvanized zinc coating process under such environment conditions.

The bond strength experiment is conducted to determine the effect of corrosion on the bond strength between the concrete and reinforcement steel for both uncoated and zinc coated steel rebar specimens embedded in cylindrical concrete.

Physical properties of steel rebar will be analyzed by investigating the Rockwell hardness, and Vickers hardness of each sample immersed in solutions of different pH and salinity as corrosive environments. Depending on the Rockwell and Vickers hardness values, the tensile and yield strength will be determined. The results will compare with the company results for a clean steel rebar.

CHAPTER II

Background

2.1 Galvanic corrosion

Galvanic corrosion is an electrochemical reaction of a metal with its environment. The term corrosion is derived from the Latin *corroder* (to eat away or to destroy), [1]. It first appeared in the *Philosophical Transactions* in 1667. The works of Plato (427-347 B.C.) contained the first written description of corrosion. Plato defined rust as the earthy component separating out of the metal., [1].

More broadly, corrosion is defined as "the deterioration of a material's properties due to its interaction with its environment.", [2]. Galvanic corrosion involves an oxidation reaction, which is anodic and produces electrons and a reduction reaction which is cathodic and consumes electrons; both oxidation and reduction reactions occur at the same time and the same overall rate, [2].

When two dissimilar metals are in contact with each other under a corrosive environment, a galvanic couple exists. The metals have different electrical potentials in the galvanic series, so the more active metal becomes an anode and corrode faster while the more noble metal becomes a cathode and is protected. There are two main factors

effecting galvanic corrosion: (1) the difference in potential between two metals in galvanic series, and (2) the size of the exposed cathodic area of the metal relative to the anodic area. The corrosion of the anode becomes faster and more damaging when the potential difference increases and also the exposed area of the cathode increase comparing to the anodic area of the metal., [3].

Reactions in which the species undergo a change in their valence electrons along with the addition or removal are called electrochemical reactions.

For example - precipitation of iron hydroxide, $Fe(OH)_2$ by electro chemical reaction is created by oxidation of metallic iron and by reduction of dissolved oxygen.

Galvanic corrosion implies two half-cell reactions; one of them is an oxidation reaction at the anode and the other is a reduction reaction at the cathode, [4]. The half-cell reaction for the corrosion of iron in water is as follows:

Anode reaction: $2Fe \Rightarrow 2Fe^{2+} + 4\ e^-$ (1)

Cathode reaction: $O_2 + 2H_2O + 4\ e^- \Rightarrow 4OH^-$ (2)

Basic components for electrochemical corrosion cell are as follows:

1. An anode.
2. A cathode.
3. A conducting environment for ionic movement (electrolyte).
4. Connection between the anode and cathode for the flow of electron current.

These components play a vital role in electrochemical corrosion; if any one of these components is disabled, the process would be stopped, [5].

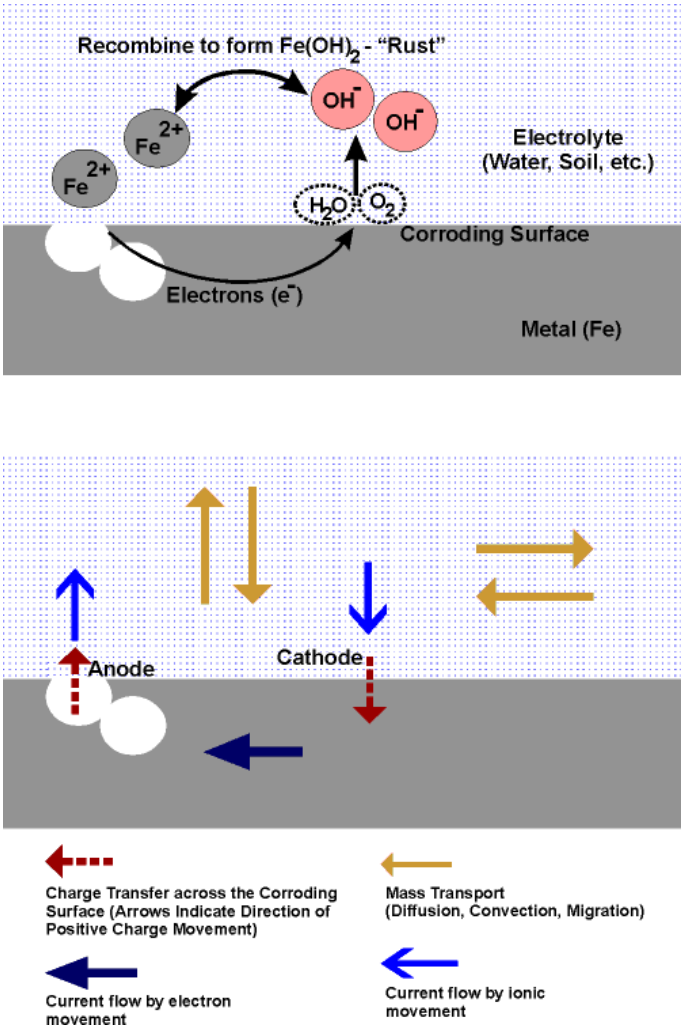

Figure 2.1 Schematic representation of electrochemical corrosion process, [6]

2.2 Electrochemical cell (Galvanic cell)

An electrochemical cell is an apparatus used for generating an electromotive force (voltage) and current from chemical reactions. The reactions releasing and receiving electrons result in flow of a current through the circuit. Oxidation occurs at the electrode called the anode which has a positive charge attracting the anions towards it; reduction

occurs at the electrode called cathode which has a negative charge attracting the cations towards it. Standard 1.5 volt battery is an example of an electrochemical cell which demonstrates Daniel cells, [7].

$$Zn \mid Zn^{2+}(c_1 mol.l^{-1}) \parallel Cu^{2+}(c_2 mol.l^{-1}) \mid Cu$$

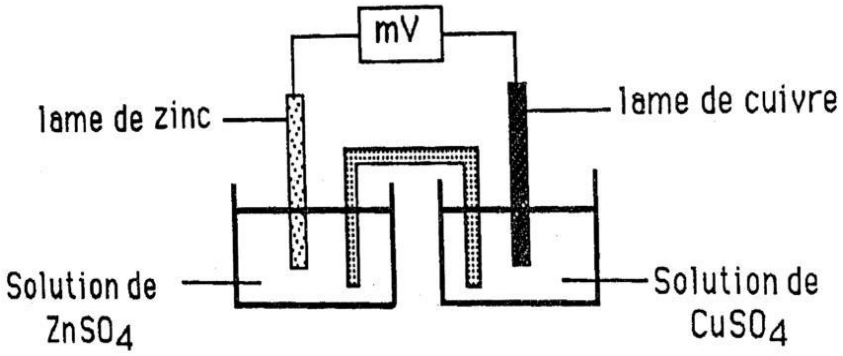

$$Zn\ (sd) + Cu^{2+} \leftrightarrow Zn^{2+} + Cu\ (sd)$$

Figure 2.2 Model of Daniel cell, [7]

2.3 Types of corrosion

Depending on the morphology of attack, the corrosion is classified into the following categories, [1]:

1. Uniform corrosion: ASTM defined the uniform corrosion as "Corrosion that proceeds at about the same rate over a metal surface", [8].
2. Galvanic corrosion: It occurs when two dissimilar metals are attached together in the presence of an electrolyte due to the difference in their electrochemical potential, [9].
3. Erosion corrosion: It can be defined as a combination result of electrochemical corrosion and mechanical wear processes, [10].

4. Fretting corrosion: It is a result of the combined actions of a corrosive environment and micro-displacements fretting wear, [11, 12].
5. Crevice corrosion: It is a form of localized electrochemical corrosion that occurs in crevices and under-shielded surfaces where stagnant solutions can exist, [13].
6. Pitting corrosion: It is a form of localized corrosion in the presence of electrolyte and produces pits or cavities on the metal surface, [14].
7. Cavitations' damage: This type is caused by the formation and collapse of air bubbles or vapor-filled cavities in a liquid near a metal surface, [15].
8. Intergranular corrosion: It is a corrosion attack that is adjacent to the grain boundaries of an alloy, [16].
9. Stress corrosion: It is a cracking of metal caused by the combined effects of a tensile stress and a specific corrosion environment acting on the metal, [17].
10. Hydrogen damage or Corrosion fatigue: It refers to the situation in which the load carrying capacity of a metallic component is reduced due to the interaction with atomic hydrogen (H) or molecular hydrogen (H_2), [18, 19].

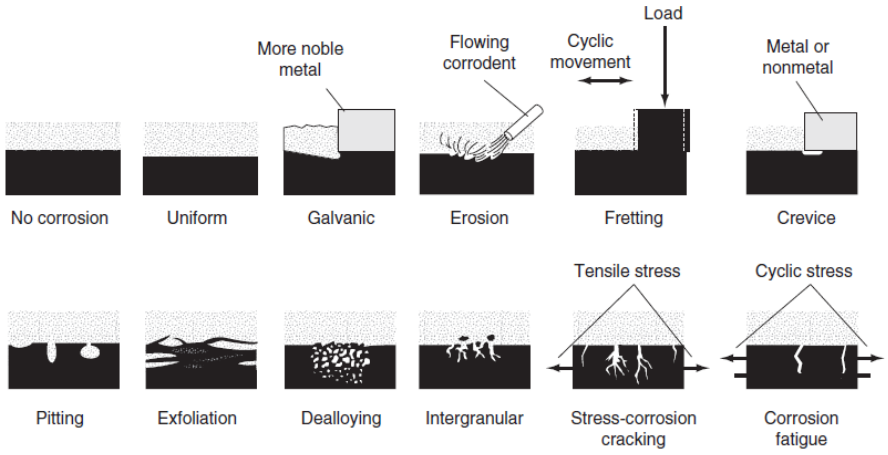

Figure 2.3 Types of corrosion, [20]

2.4 Corrosive environments

Corrosive environments are generally classified as an atmospheric, underground/soil, water, acidic, alkaline, and combinations of these. All environments are corrosive to some degree, and they are broadly classified as, [21]:

1. Air and humidity.
2. Fresh, distilled, salt and marine water.
3. Natural, urban, marine and industrial atmospheres.
4. Steam and gases, like chlorine, Ammonia.
5. Hydrogen sulfide.
6. Sulfur dioxide and oxides of nitrogen.
7. Fuel gases.
8. Acids.
9. Alkalies.
10. Soils.

This study mainly concentrates on the solutions of different pH and salinity as corrosive environments, and the effect of these environments on the corrosion of reinforced concrete and its bond strength.

2.4.1 The effect of pH

The pH affects the iron metal in an aerated water environment as explained below, formation of ferrous oxide as follows:

Reduction reaction in the aqueous solution (Cathodic reaction)

$$O_2 + 4e^- + 2H_2O \rightarrow 4OH^- \quad (3)$$

Oxidation reaction of the iron metal (Anodic reaction)

$$2Fe \rightarrow 2Fe^{2+} + 4e^{-} \quad (4)$$

Overall reaction in aqueous solution

$$Fe^{3+} + 3H_2O \rightleftharpoons Fe(OH)_3 + 3H^{+} \quad (5)$$

$$Fe(OH)_3 \rightleftharpoons FeO(OH) + H_2O \quad (6)$$

$$2FeO(OH) + O_2 \rightleftharpoons Fe_2O_3 + H_2O \quad (7)$$

At a range of pH below (4) i.e. in acidic medium, the diffusion barrier oxide film (Fe_2O_3) dissolves, exposing the metallic iron with the aqueous solution, which results in increasing the rate of corrosion of iron. This is mainly due to the evolution of hydrogen ions, and at low pH, oxygen is not controlling the corrosion process. The range of pH between (4 and 10) affects the rate of corrosion depending at the rate of diffusion of oxygen to the cathodic surface. For pH greater than (10), the rate of corrosion decreases due to the formation of a passive layer over the metallic iron. The passive layer is formed in the presence of dissolved oxygen and alkalizes, [20].

2.4.2 The effect of salinity

Depending on the concentration of dissolved salts in the water, it is called hard or soft water. Higher concentration of salts in water is called hard water, if not it's called soft water. Initially, an increase in concentration of salt increases the rate of corrosion due to presence of dissolved oxygen. After a certain point, the corrosion rate decreases linearly due to the decrease in solubility of oxygen at high salt concentration, [20].

2.5 Corrosive environment in Iraq

Iraq is almost completely landlocked; the area around Umm Qasr offers Iraq's only access to the Arab Gulf. The area consists of three ports and terminals: Al Basrah, Khawr az Zubayr, and Umm Qasr. Iraq has two major rivers which are the Euphrates River (2,815 km) and the Tigris River (1,899 km), as well as the third River (565 km) which is manmade waterway to serve as a major irrigation drainage canal. Other Iraqi small rivers include Diyala River, Great Zab River, and Little Zab River. Iraq also has many other water bodies such as lakes and marshes. Lakes are located in northern and central Iraq, while marshes are located in the south. Euphrates and Tigris Rivers, which are flowing from northern part to southern part of Iraq, provides 98% of water supply in the country. Along the rivers, there are a lot of bridges and hydraulic structures which need to be protected. The quantity and quality of water in these rivers change with seasons and positions. During the wet season, the quality of water is good near its sources, but it gets poor when it flows down to the south especially in the summer season. Nearby, across, or in previously mentioned Iraqi water bodies, there are several structures that need to be protected from corrosion effects. Those structures may include, but are not restricted to bridges, dams, and buildings.

Far from water bodies, structures and buildings suffer from other causes of corrosion, which are the high water table and the salinity of ground water. The salinity of the soil and so as ground water increases from Baghdad south to the Arabian Gulf, such phenomena may relate to the poor surface and subsurface drainage, and the irrigation method used is mostly gravity irrigation. The situation is particularly critical in Basra

(southern Iraq) where salinity may exceed 7,000 PPM (the World Health Organization standard for human consumption is 500 PPM or less), [22, 23].

2.6 Corrosion of reinforced concrete

Concrete is mainly a reaction product of cement, water and other aggregates. Concrete has good compressive strength but very poor tensile strength; rebars are embedded in the concrete to improve the tensile strength capability. Such type of concrete element is called reinforced concrete, [24]. Steel is thermodynamically unstable in the earth's atmosphere, so it always tends to form an oxide or hydroxide by reacting with oxygen and water, [25].

Rebar corrosion causes reduction of its cross section area, which minimizes the tensile strength bear, such phenomena, which is conjugate with the rust result due to corrosion, leads to reduce the bond strength between the steel and the concrete, [26]. The major cause for initiation of the reinforced concrete corrosion process in marine environment is the reaction of dissolved oxygen on the steel surface which produces iron oxides and hydroxides. These products get accumulated in the concrete around the steel. This accumulation within a constrained space will develop an additional stress with a crack in the concrete cover, which results in progressive damage to the concrete, [27]; for example the reinforced concrete bridges across the river (Fig. 2.4). As a result of corrosion, the reinforced concrete has a very short lifetime of structures, which needs more financial support for its replacement thus decreasing its economic value, [20].

Figure 2.4 Corrosion of reinforced concrete in bridge

2.7 Mechanism of corrosion in reinforced concrete

For embedded steel in concrete, the steel is exposed to less oxygen and water as the concrete itself is considered as a porous medium. Also the cement paste in the concrete has a very high alkanity; at this high pH, the corrosion product formed is insoluble. The products form a protective layer (passive layer) which prevents the loss of metal from a steel surface. The protective film is formed at high value of pH that is explained in the figure 2.5.

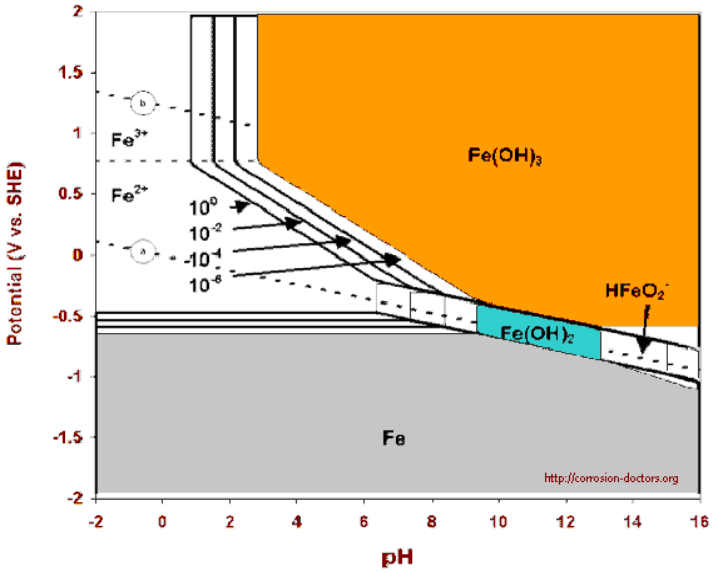

Figure 2.5 Pourbaix diagram for iron showing the potential and pH, [28]

In figure 2.5, Gray region indicates the stable steel inside the concrete, orange and green regions are the passivity regions and white regions are active corrosion sites. When the passive layer breaks down due to the intrusion of aggressive elements like chlorides and carbonation of the concrete, it results in structural deterioration, [28].

2.7.1 Passivation

Passivity is a fundamental property of a metal which resists corrosion in the given environment resulting from thermodynamic tendency to react.

Passive film is a diffusion barrier film which is insoluble and produced as a reaction product. For example, the oxide of a metal separates the metal from its corrosive environment which results in decreasing the rate of corrosion. This theory is called oxide film theory, [19]. The longer that metal stays in corrosive environment, the film becomes more stabilized, [29].

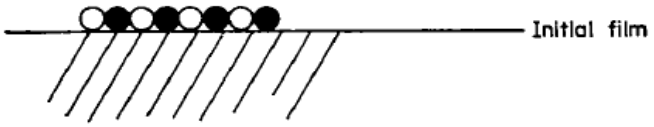

Figure 2.6 Initial passive layer containing less than monolayer of adsorbed oxygen, [20]

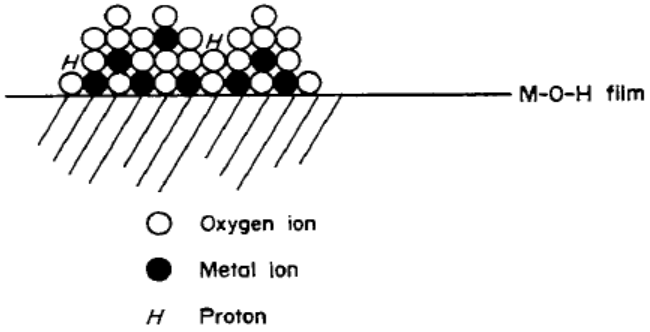

Figure 2.7 Thicker passive layer with addition metal ions and protons, [20]

2.7.2 Carbonation

Carbonation is a process in which carbon dioxide from the atmosphere reacts with water in concrete pores to form carbonic acid. This acid then reacts with alkalis in the pores neutralizing it, [30]. The alkaline constituents mainly include sodium, potassium hydroxides and solid hydration products, e. g. Ca (OH) $_2$. Alkaline products react with carbon dioxide readily to form the carbonate product. The reaction of calcium hydroxide and carbon dioxide takes place in aqueous phase as follows:

$$CO_2 + Ca(OH)_2 \xrightarrow{H_2O,NaOH} CaCO_3 + H_2O \quad (8)$$

This process does not result in corrosion of concrete, but it shrinks the concrete and thus results in corrosion of embedded steel, [24].

2.8 Corrosion protection

In corrosive environments such as a marine zone, there is a need to coat the metals with materials possessing corrosion inhibiting properties to protect the metals from corrosion. The corrosion problem is a very serious issue, especially in offshore constructions such as harbors and bridges. The most common causes for corrosion in reinforced concrete include the breakdown of the oxide film on the steel by chloride ions and of the concrete by its nature, as it reacts with the atmospheric carbon dioxide, [21].

Methods for controlling corrosion in reinforced concrete include:

1. Material selection
2. Protection by coating
3. Inhibitors
4. Cathodic protection

5. Design

2.8.1 Material selection

Materials of metals play a vital role in corrosion; each metal has its unique corrosive behavior. For example, more noble metals (gold or platinum) are highly resistant to corrosion than the more active metals (sodium or magnesium). Also it depends on the environment to which it is exposed.

2.8.2 Protection by coating

A protective coating system to prevent corrosion in reinforced concrete includes:

- Metallic coating like zinc coating.
- Non-metallic coating like bonded epoxy coating.

2.8.2.1 Zinc coating

Zinc is a bluish- white, conductive, and reactive metal. It is fragile at low temperature, but it is malleable at high temperature from 100 to 150 ^{o}C. Due to its excellent corrosion resistance property in most environments, zinc is used as a coating material for metals. In addition, it has the ability to form an adherent, and dense film or layer when it is exposed to the atmosphere. When zinc reacts with the oxygen or water, it produces a layer of zinc oxide which is insoluble in water and constitutes a barrier or parting which isolates the zinc from an aggressive environment.

As zinc has more negative potential in galvanic series than iron or steel, it becomes as an anode with the iron or steel metal (as shown in table 2.1). In galvanic corrosion, when iron acts as a cathode, zinc acts as an anode and prevents corrosion, [21].

General steps taken before coating are:

1. Wet chemical cleaning by using alkaline detergent and then drying.
2. The whole coating of the metal with zinc, and leaving it until dried.

The corrosion behavior of multilayer coating is affected by the following factors such as coating quality, presence of any fault in the coating process such as leaving some places without coating, and thickness of the coating layers, [20].

Table 2.1 Standard electromotive force (Emf) series

	Electrode Reaction	*Standard Electrode Potential, V^0* (V)
	$Au^{3+} + 3e^- \longrightarrow Au$	+1.420
↑	$O_2 + 4H^+ + 4e^- \longrightarrow 2H_2O$	+1.229
	$Pt^{2+} + 2e^- \longrightarrow Pt$	~+1.2
	$Ag^+ + e^- \longrightarrow Ag$	+0.800
Increasingly inert	$Fe^{3+} + e^- \longrightarrow Fe^{2+}$	+0.771
(cathodic)	$O_2 + 2H_2O + 4e^- \longrightarrow 4(OH^-)$	+0.401
	$Cu^{2+} + 2e^- \longrightarrow Cu$	+0.340
	$2H^+ + 2e^- \longrightarrow H_2$	0.000
	$Pb^{2+} + 2e^- \longrightarrow Pb$	−0.126
	$Sn^{2+} + 2e^- \longrightarrow Sn$	−0.136
	$Ni^{2+} + 2e^- \longrightarrow Ni$	−0.250
	$Co^{2+} + 2e^- \longrightarrow Co$	−0.277
	$Cd^{2+} + 2e^- \longrightarrow Cd$	−0.403
	$Fe^{2+} + 2e^- \longrightarrow Fe$	−0.440
Increasingly active	$Cr^{3+} + 3e^- \longrightarrow Cr$	−0.744
(anodic)	$Zn^{2+} + 2e^- \longrightarrow Zn$	−0.763
	$Al^{3+} + 3e^- \longrightarrow Al$	−1.662
↓	$Mg^{2+} + 2e^- \longrightarrow Mg$	−2.363
	$Na^+ + e^- \longrightarrow Na$	−2.714
	$K^+ + e^- \longrightarrow K$	−2.924

2.8.2.2 Epoxy coating

Epoxy resin is formed as a result of copolymerization of an epoxide with another compound having two hydroxyl groups. It is mainly used as a thermosetting resin, coatings, and adhesives. The general procedures for epoxy coatings are as follows:

1. Pretreatment the surface by shot blasting at a temperature of 120-130 ^{o}C.
2. Electrostatic spraying.
3. Curing for 20 minutes at surface temperature of 200 ^{o}C, [31].

2.8.3 Inhibitors

In the coating process, inhibitors are incorporated as a protective cover or as a primer for the coating. When there is a defect in the coating, the inhibitor leaks from the coating and controls the corrosion. Common examples of inhibitors are Chromates, silicates, and organic amines, [21].

2.8.4 Cathodic protection

Cathodic protection is one of the most effective and common methods to prevent or control corrosion in many metals, especially the rebars in reinforced concrete. It involves the application of voltage. In cathodic protection, the electrons will flow from the more negative potential (more active metal) to the less negative potential (more noble metal). The more negative potential -which is the anode- corrodes, whereas the less negative potential -which is the cathode- remains protected, [32].

The important factors that influence the cathodic protection are as follows:

- Anode life time: the longer the life times of an anode, the more effective the system of cathodic protection.

- Current distribution: When current flows directly from the anode to the cathode without distributing out of the system, the cathode is more protected.
- Anode's compatibility with surrounding materials and its installation, [32].

2.8.5 Design

Proper designing for structures and equipments can reduce the effect of corrosion to a great extent. Reducing corrosion effect by adopting a proper designing procedure can be achieved through many ways; such ways may include, [9]:

- Selection of metals with minimum difference in electrode potential whenever dissimilar metals is necessary.
- Whenever possible, it is best to use butt joints rather than lap joints.
- Using drip irrigation to prevent water gathering down buildings.
- Using sealants at joints and connections to prevent moisture entering.
- In hydraulic structures, it is better to avoid the flow turbulence by avoiding sudden change in direction or section of the flow path.
- Provide standby equipments for the critical systems, such as ventilation system, thermal radiator, pumps, and others.
- Using nonmetallic materials whenever possible.

2.9 Economical impact of corrosion

The effect of corrosion is a worldwide economic problem. Such economical impacts need a replacement of the corroded equipment or its parts, and suitable corrosion protection methods. They may also lead to a decrease of efficiency, a damage of

equipment, an increase of environmental impact due to the increase of pollutant emission or spilling of hazard materials, and an increase of the need of over design to provide appropriate corrosion allowance, [1].

Besides the economic importance of corrosion, two other aspects that make corrosion control an important consideration are conservation and human safety. Life-cycle analysis studies estimate the indirect cost of corrosion for highway bridges due to traffic delays to be ten times the direct cost of corrosion, [33]. Because of this economic cost, many production and manufacturing companies, state and federal highway agencies, and infrastructure developers are pursuing corrosion protection methods for reinforced concrete structure and equipment.

CHAPTER III

Experimental Methods

3.1 Introduction

This chapter describes the materials, equipment and methods that are necessary to perform the experiments for this study. This study focuses on three sets of experiments which include the investigation of the effect of pH and salinity of the surrounding environment on the corrosion rate of reinforced concrete, on the physical properties of steel rebar, [34] and on the bond strength between the rebar and the concrete element. The experiments also determine the effect of the cold galvanized zinc coating process in reducing the corrosion rate of the rebar, as well as determine the effect of this corrosion protection method on the bond strength.

Physical properties of the reinforcing steel rebar that were studied are Rockwell hardness, Vickers hardness, yield strength and tensile strength. The results were then compared with the standard properties that have been obtained from the supply company for the rebar. The corrosion rate tests were conducted using the Tafel test method and weight loss method. Furthermore, the bond strength test was examined by using material test system.

3.2 Materials

The rebar used in this study was purchased from Stillwater Steel and Welding Supply Company. Concrete elements were prepared in the structure lab at civil engineering department at OSU. Professional cold galvanizing compound zinc spray was purchased from Ag Distributors & Supplies Corporation Company. Chemicals like Sodium hydroxide (NaOH), Sodium chloride (NaCl) and Hydrochloric acid were bought from Sigma Aldrich. Plastic containers of specific sizes to hold the samples and labels were purchased from the chemistry store at OSU. Distilled water was available in the chemical engineering department at OSU and glue sticks were purchased from Wal-Mart for experimental purpose.

3.3 Equipment

Equipment used in this study includes corrosion tester, Rockwell hardness, Vickers hardness, and polishing equipment are available at mechanical engineering lab at OSU. The digital balance and pH-meter are accessible in chemical engineering lab (410). Material test system is available at structure lab of civil engineering department at OSU.

3.4 Experimental methods

Three sets of experiments were performed; those experiments may be categorized as follows:

3.4.1 Physical properties of the steel rebar

This set of experiments was designed to investigate the effect of corrosion rate on the physical properties of the rebar. The rebar is characterized by two tests namely Rockwell Hardness (HRC), and Vickers Hardness (HV).

All rebar (type #4) used for these tests have the same dimensions which are 0.5 inch (13 mm) diameter and 4 inch (101.5 mm) length . The supplier report that provides chemical analysis and physical properties of the used rebar is attached in Appendix A.

Ten cylindrical reinforced concrete elements were prepared; five of those were immersed in solutions of different pH (4, 6.7,10,12 and 14) at a temperature of 23°C. The pH was adjusted with the use of 0.1 HCl, 0.02N NaOH and distilled water. The remaining five samples were immersed in solutions of different salt (NaCl) concentration of (3, 6, 9, 12, and 15) g/L at 23°C.

Ten prepared samples of reinforced concrete with their solutions of different pH and salt concentration are shown in figure 3.1.

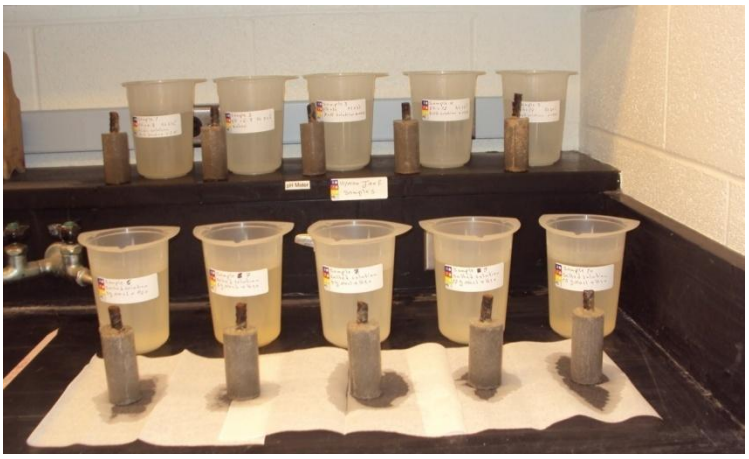

Figure 3.1 Prepared cylindrical reinforced concrete element

The samples were left undisturbed for three months. After three months, the concrete elements were then smashed and the rebar recovered. The rate of corrosion at the surface of the steel rebar inside the concrete was negligible; whereas, the corrosion at

the surface exposed to the corrosive solution was considerable. The steel rebar of ten samples after three months are shown in figure 3.2.

Figure 3.2 Steel rebar that was recovered after 3 months period

The exposed part of the steel rebar was subjected to series of tests which include Rockwell hardness (HRC) and Vickers hardness (HV). The procedures for calculating Rockwell hardness and Vickers hardness are summarized as follows:

3.4.1.1 Rockwell hardness

The purpose of this test is to measure the Rockwell hardness of rebar embedded in concrete element immersed in different pH and salt concentration solutions and to compare the results with the specifications obtained from the rebar supplier report. The procedures for conducting the Rockwell hardness test should follow certain conditions. The hardness is measured according to the depth of indentation under a constant load. Also, the loading speed should be standardized. Furthermore, the surface to be tested should be smooth, clean, dry and free from oxides. The Rockwell number represents the

increment in depth from the zero reference position to the final increment position based on the applied load, [35].

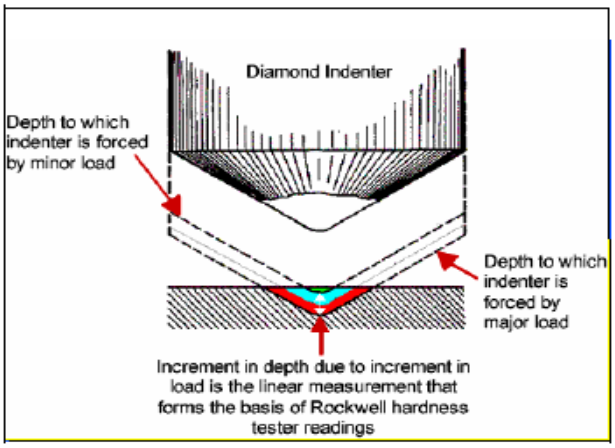

Figure 3.3 Rockwell hardness indenter

The test is conducted by applying 150 Kg force on the specimen in the CLARK CR Series Rockwell hardness tester for few seconds, and the tester automatically generates the value of Rockwell hardness. A CLARK CR Series Rockwell hardness tester is shown in Figure 3.4.

Figure 3.4 CLARK CR Series Rockwell hardness tester

Tensile strength can be determined using HRC results depending on Table (B-1) at Appendix (B), [36, 37]. The (HRC) used in this study is type (C) using 150 kg load.

3.4.1.2 Vickers hardness

The purpose of this test is to investigate the Vickers hardness of the same ten rebar which were used to find the Rockwell hardness and to compare the results with the company value of the clean rebar. Vickers hardness number is defined as a ratio of the load divided by the surface area of the indentation. Vickers hardness tester uses a square-base diamond pyramid as the indenter with the included angle between opposite faces of the pyramid at 136°, [35]. Vickers instrument with its indenter is shown in figure 3.5.

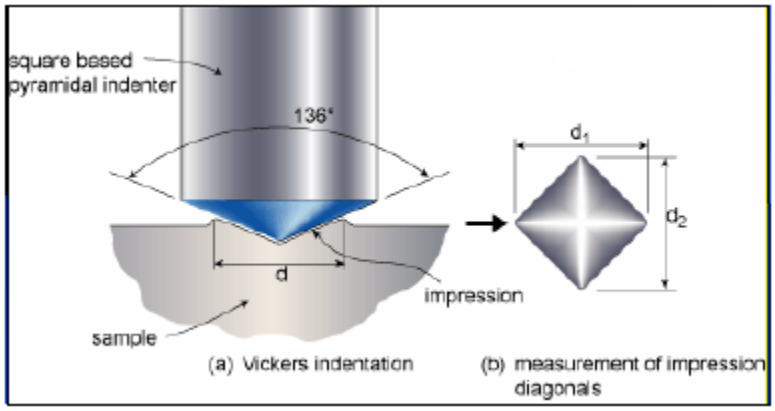

Figure 3.5 Vickers Instrument

The samples should be polished before proceeding to the test. Figure 3.6 shows the polishing process which includes the following three steps:

First Step - polishing the sample using Carbimet paper (strips 320 Grit).

Second Step - polishing the sample using Buehler Carbimet (sheets 600 Grit).

Third Step - polishing the sample by using the Buhler machine Micro polish with (0.3 micron Alpha Alumina).

(a) (b) (c)

Figure 3.6 Polishing equipment and polished samples (a) First and second steps (b) Third step (c) The polishing sample

After the polishing steps, the Vickers hardness was measured by using CLARK model CM-400AT Vickers hardness tester. By applying 200 Kg force on the small piece of the specimen for 15 seconds, the CM-400AT Vickers hardness tester gives the value of Vickers hardness. Clark model CM-400AT Vickers hardness tester is shown in Figure3.7.

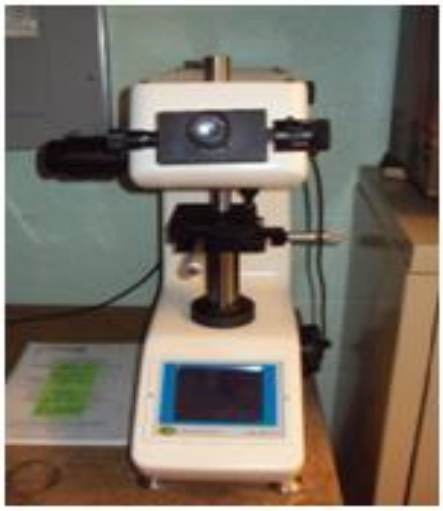

Figure 3.7 Clark model CM-400AT Vickers hardness tester

Yield strength can be determined by using the test results of (HV). The correlation related (HV) and yield strength (Y) is known as Tabor relation, [38, 39] who states that:

$$Y = \frac{HV}{3} \quad (1)$$

3.4.2 Corrosion rate of reinforced concrete

In this study, two methods were used to measure the corrosion rate of the rebar that were subjected to corrosive environment. The first one was Tafel test method which is considered as a time saving method due to the short time required to obtain the result. The second one was the weight loss method which requires measuring the weight of the rebar at the beginning and the end of the experiment.

3.4.2.1 Tafel Test method

Tafel extrapolation method is an electrochemical technique for corrosion measurement, [40]; electrochemical test method is popular because it can be carried out in a short period of time, [41]. Julius Tafel (German chemist 1862-1918), [42] introduced the following equation that governs the voltage-current characteristic of the liquid-solid interface as follows, [43]:

$$\eta = \frac{RT}{\alpha F}\ln i_o - \frac{RT}{\alpha F}\log i \quad (2)$$

Where η is the potential difference ($E_c - E_a$), i is the current, i_o is the exchange current, F is the faraday's constant in the absolute temperature, R is the gas constant and α is dimensionless parameter with values between 0 and 1; this is often estimated to be 0.5.

Tafel equation is reduced to a simple form that represents a single electrode with respect to a reference electrode as follows, [43]:

$$\eta = a + b \log i \quad (3)$$

Where a and b are constants that can be easily inferred from equation (2). A graphical representation of log $|i|$ versus η is known as a Tafel plot.

The experimental procedures for carrying out the Tafel test are as follows:

A steel rebar (#4) of 1 inch (25.4 mm) diameter was used to carry out the experiment. The samples were cut into circular sections, and then the circular samples were refined and polished using polishing apparatus. The polishing apparatus and the circular samples are shown in Figure 3.8.

Figure 3.8 The polishing apparatus and the circular samples

The polished circular sample was then seated on the opened side of the corrosion tester cell (Figure 3.9) and sealed with screw in order to prevent the leakage of electrolyte during the experiment. In the corrosion tester device, the circular sample was the anode which is the working electrode while a solid piece of platinum located at the other end of

the cell is the counter electrode. In addition, a saturated (Ag-AgCl/KCl) is the reference electrode that has constant potential and the sensor is the fourth electrode.

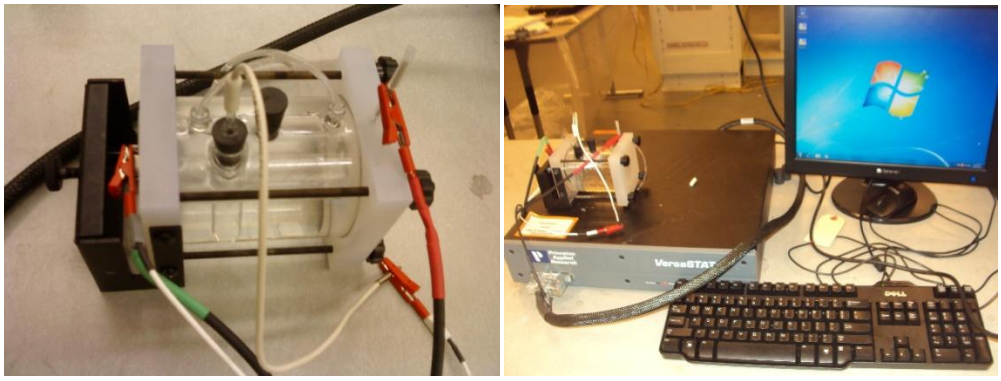

Figure 3.9 Corrosion tester connected with the computer

The electrolyte of the cell was prepared depending on ten different sets of corrosive conditions which are listed below:

1. Acidic solution of (0.1 N) HCl with pH =2 used for sample 1.
2. Acidic solution (0.1 N) HCl with pH=4 used for sample 2.
3. Distilled water with pH=7 used for sample 3.
4. Alkaline solution of (0.02N) NaOH with pH=10 used for sample 4.
5. Alkaline solution of (0.02N) NaOH with pH=12 used for sample 5.
6. Saline solution with NaCl concentration = 3g/L used for sample 6.
7. Saline solution with NaCl concentration = 6g/L used for sample 7.
8. Saline solution with NaCl concentration = 9g/L used for sample 8.
9. Saline solution with NaCl concentration = 12g/L used for sample 9.
10. Saline solution with NaCl concentration = 15g/L used for sample 10.

After pouring the electrolyte inside the cell from a hole at its top, the hole was sealed and then the electrodes were connected. The corrosion tester device was switched

on, and the Tafel program was run on the computer. The Tafel program requested information about the samples under examination, such as the type of anode (which was a solid substance), the type of the reference electrode (which was a saturated Ag-AgCl/KCl), the density and the equivalent weight of the steel rebar used. The selected area of the examination was 1 cm^2 with the primary potential of (-1.1 V) and the final potential of (-0.5 V), which is the standard potential for the examination of steel. Finally, the duration of each reading was specified as three seconds. The sketch of the corrosion tester cell is shown in figure 3.10.

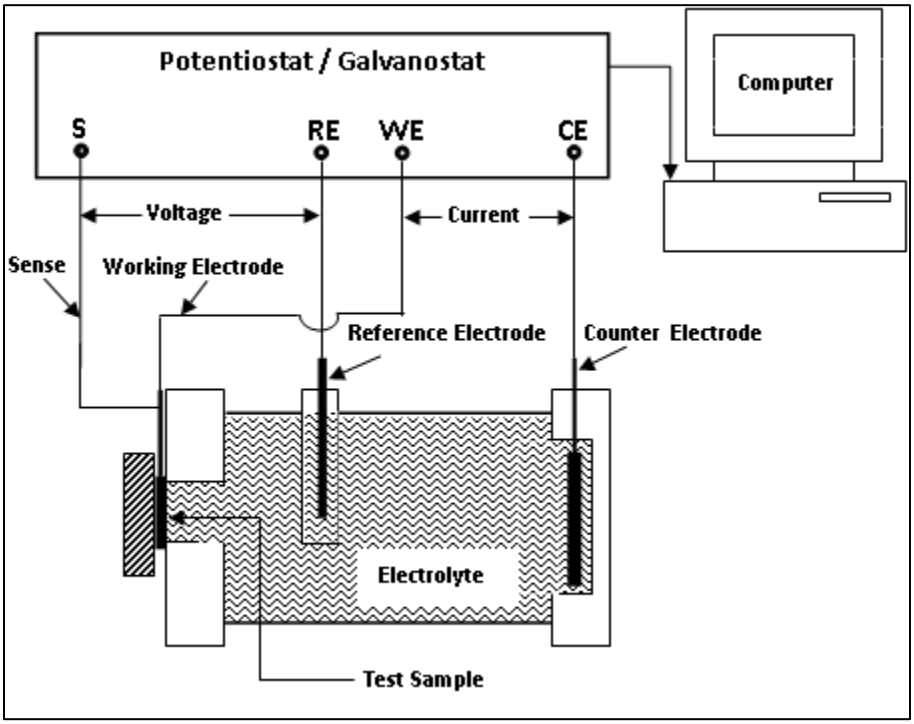

Figure 3.10 The corrosion tester cell

The experiment required one hour completing and the final results appeared as a Tafel plot of potential vs. current. Corrosion rate and corrosion current density (I_{corr}) values were also given.

The current density is defined as Stern-Geary equation which is stated that:

$$I_{corr.} = \frac{1}{R_p}\left[\frac{\beta_a \beta_c}{2.3\,(\beta_a \beta_c)}\right] \quad (4)$$

Where $I_{corr.}$ is the corrosion current density in (A/cm^2), R_p is the polarization resistance (ohm. cm^2), and β_a , β_c are the anodic Tafel and the cathodic Tafel coefficients.

The corrosion tester software is calculated $I_{corr.}$ directly by applying equation (4) when R_p is negligible in this test because it is very small, and then the program computed the corrosion rate (C_R) directly using the following equation:

$$C_R\ (\text{mpy}) = \frac{0.13 * I_{corr.} * (E.W.)}{d} \quad (5)$$

Where $E.W.$ is the equivalent weight of the sample in (g/mol), d is the density of the sample in (g/cm$^{3)}$, and C_R is the corrosion rate in milli-inches per year (mpy).

To know how the resistance can affect the corrosion rate; equation (4) can simplify to the following formula:

$$\frac{I}{A} = \frac{\beta}{R_p} \quad (6)$$

Where I and β are the current (ampere) and the Tafel coefficient respectively, while A is the cross sectional area of the metal that expose to the electrolyte (cm^2).

$$A = r^2 * \pi$$

From eq. (6), the cross sectional area (A) is positively proportion to the polarization resistance, so they are both inversely proportion to $I_{corr.}$ and the corrosion rate.

The polarization resistance can be written as follows:

$$R_p = \rho * L \quad (7)$$

Where ρ is the electrical resistivity of a metal that has a unit (ohm. m) and is also called the specific resistance, and L is the distance between the working electrode and the reference electrode (m).

From eq. (7), the polarization resistance is positively proportion to the metal resistivity, so they are both inversely proportion to the corrosion rate.

3.4.2.2 Weight loss method

The corrosion rate in this method is determined by calculating the weight loss of the rebar due to exposure to corrosive environment. Thirty samples of cylindrical concrete with embedded rebar were prepared to carry out the experiment set. Each rebar specimen had a diameter of 0.5 inch (12.7 mm) and a length of 4 inch (101.6 mm).

Fifteen of the rebar were coated with the zinc while the other fifteen were left uncoated, [44]. Ten samples from each group of uncoated and coated were immersed in solutions with different pH at temperature 23°C. The pH ranges were as follows:

1. Sample No 1 from uncoated and coated groups were immersed in solution with pH=1.5, which was prepared using acidic solution containing 100 ml HCL in 1000 ml water.
2. Sample No 2 from uncoated and coated groups were immersed in solution with pH=2.1, which was prepared using acidic solution containing 80 ml HCL in 1000 ml water.
3. Sample No 3 from uncoated and coated groups were immersed in solution with pH=2.6, which was prepared using acidic solution containing 60 ml HCL in 1000 ml water.

4. Sample No 4 from uncoated and coated groups were immersed in solution with pH=3.2, which was prepared using acidic solution containing 40 ml HCL in 1000 ml water.
5. Sample No 5 from uncoated and coated groups were immersed in solution with pH=4.3, which was prepared using acidic solution containing 20 ml HCL in 1000 ml water.
6. Sample No 6 from uncoated and coated groups were immersed in distilled water with pH=7.2.
7. Sample No 7 from uncoated and coated groups were immersed in solution with pH=10.3, which was prepared using alkaline solution containing 25 g NaOH in 1000 ml water.
8. Sample No 8 from uncoated and coated groups were immersed in solution with pH=11.5, which was prepared using alkaline solution containing 50 g NaOH in 1000 ml water.
9. Sample No 9 from uncoated and coated groups were immersed in solution with pH=12.8, which was prepared using alkaline solution containing 75 g NaOH in 1000 ml water.
10. Sample No 10 from uncoated and coated groups were immersed in solution with pH=13.9, which was prepared using alkaline solution containing 100 g NaOH in 1000 ml water.

The Other five samples from each group of uncoated and coated were immersed in NaCl solutions of different concentration at a temperature of 23°C. The salinity concentration was as follows:

11. Sample No 11 from uncoated and coated groups were immersed in solution with salinity (NaCl) concentration = 10g/L.
12. Sample No 12 from uncoated and coated groups were immersed in solution with salinity (NaCl) concentration = 20g/L.
13. Sample No 13 from uncoated and coated groups were immersed in solution with salinity (NaCl) concentration = 30g/L.
14. Sample No 14 from uncoated and coated groups were immersed in solution with salinity (NaCl) concentration = 40g/L.
15. Sample No 15 from uncoated and coated groups were immersed in solution with salinity (NaCl) concentration = 50g/L.

The zinc coating product that was used in this study is professional cold galvanizing compound zinc spray. The zinc coating product and the coated rebar are shown in figure 3.11 (a) and 3.11 (b) respectively.

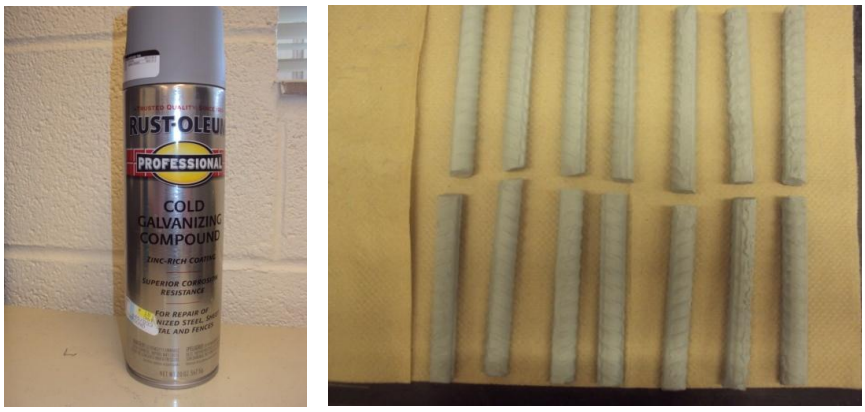

(a) **(b)**

Figure 3.11 (a) the zinc coating product (b) The coated rebar

The thirty prepared reinforced concrete samples consisting of fifteen uncoated and fifteen coated are shown in Figure 3. 12 (a) and 3.12 (b) respectively.

(a) **(b)**

Figure 3.12 Prepared samples (a) uncoated (b) coated

After three months time period, these thirty samples were smashed and the steel rebar were digging out. One inch length of the steel was cut from extracted rebar, which was exposed to the solution directly, to avoid the corrosion that happened due to the corrosive solutions. Therefore, we consider just the corrosion that happened on the part of steel rebar that was inside the concrete element which was three inch length. All calculations of weight and weight loss were taken per inch of steel rebar. The uncoated and coated steel rebar after three months are shown in figure 3.13 (a) and (b) respectively.

(a)

(b)

Figure 3.13 Steel rebar after 3 months period (a) uncoated (b) coated

The weight loss of the rebar can be used to calculate the corrosion rate as a micrometer / year (µm/year) using the following equation:

$$C_R\left(\frac{\mu m}{year}\right) = 8.76 * 10^7 \frac{w}{A*T*D} \quad (8)$$

Where: C_R is the corrosion rate in $\left(\frac{\mu m}{year}\right)$, W is weight loss (g), A is the contact area of steel specimen (cm^2), T is the exposure time (hr), and D is density of steel (7.8g /cm3).

Contact area of specimen may be calculated using the following equation:

$$A = 2(3.14)*(r^2) + 2(3.14)*r*h \quad (9)$$

Where h is the contact length of the rebar specimen, and r is the radius of the rebar.

3.4.3 Bond strength test

The purpose of this experiment is to investigate the effect of corrosion on the bond strength between the concrete and reinforcement steel for both uncoated and zinc coated steel rebar specimens that were embedded in cylindrical concrete, [45]. These samples were immersed in solutions having different pH and different salinity concentration. This experiment helps in determining the relation between the pH of the surrounding medium (pH range = 1-14) and the maximum allowable shear stress required to cause failure of bond strength between the concrete and the steel rebar. Also, it determines the relation between the salinity of the surrounding medium and maximum allowable shear stress required to cause failure of bond strength between the concrete and the steel rebar during the test.

The steel rebar, which was used to carry out the experiment, has the dimensions of 0.5 inch (12.7 mm) diameter and 5 inch (127 mm) length.

Thirty cylindrical reinforced concrete elements were prepared; fifteen of them were coated with the zinc while the other fifteen were left uncoated. The zinc coating product that was used to carry out the coating process is as the same product as in experiment of weight loss method; as shown in figure 3.11.

The thirty concrete samples that included uncoated and the zinc coated rebar had the dimensions of 3 inch (7.62 cm) diameter and 3 inch (7.62 cm) depth. Four holes were made on each of the thirty samples by embedding four glue sticks on the concrete mortar parallel to the rebar direction and at same distance from the rebar. These holes were made in order to allow the chemical solution to penetrate inside the concrete element, to be closer to the rebar, and then to accelerate the corrosion process within the period of

three months. The prepared concrete samples with embedded rebar are shown in figure 3.14.

Figure 3.14 Prepared cylindrical concrete samples with embedded rebar

Ten samples from each group of uncoated and coated were immersed in solutions with different pH at temperature 23°C. The Other five samples from each group of uncoated and coated were immersed in Nacl solutions with different concentration at a temperature of 23°C. The pH range and the salt concentration were as the same as the weight loss method. Some of these samples with their solutions were shown in Figure 3.15.

Figure 3.15 Samples with different pH and salinity concentration

After three months time period, these thirty concrete samples were removed from their immersed solutions in order to conduct the bond strength test. The bond strength test was carried out using a computerized material test machine which is shown in figure 3.16, [46].

Figure 3.16Computerized Material Test System used to carry out bond strength test

Figure 3.17 (a), (b), (c), and (d) shows different tools that were used during the bond test and different views during the test.

(a) Rebar's catcher cylinder

(b) Fixed steel box (right), downward moving steel box(left)

(c) Beginning of the test

(d) End of the test

Figure 3.17 Tools used during the bond strength test and different views

Figure 3.18 represents a sketch that illustrates the arrangements of steel boxes, catcher cylinder, and concrete sample during the test.

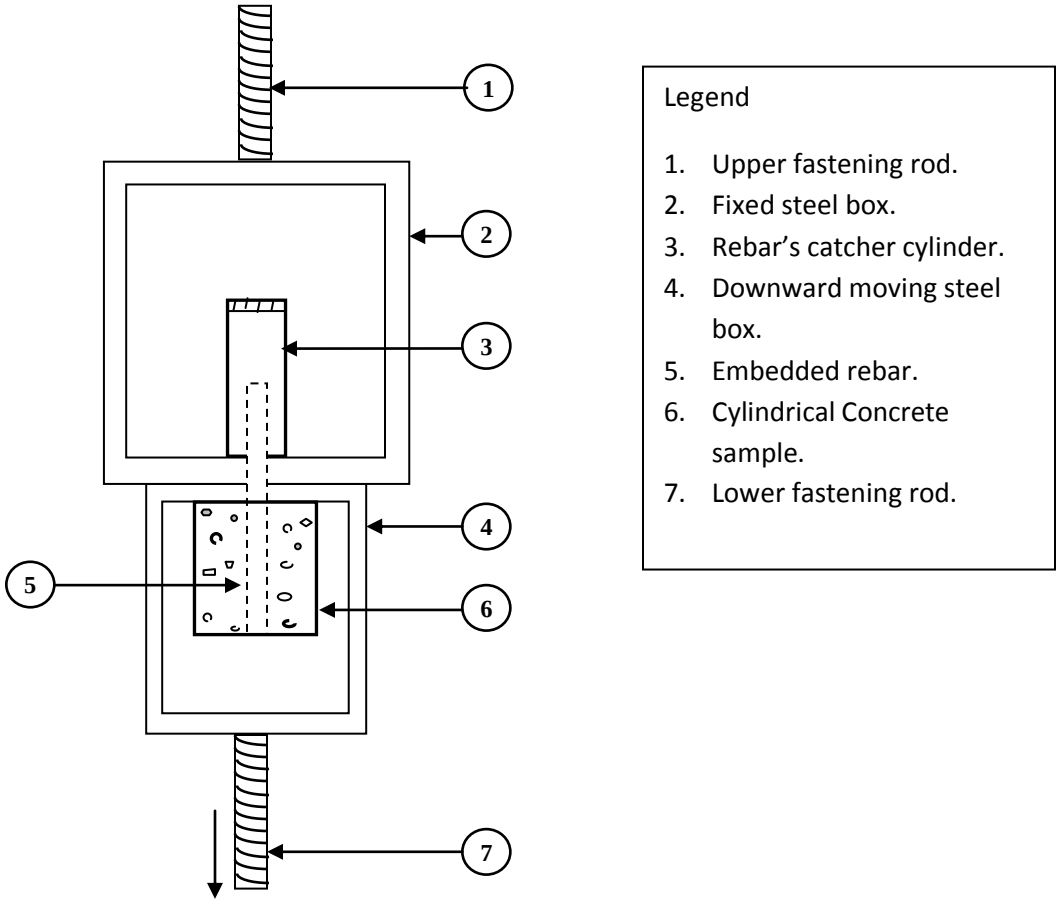

Figure 3.18 Arrangements of steel boxes, catcher cylinder, and concrete sample during the test

The bond strength test was carried out for all thirty samples after three months using the material test system. The test was applied by setting up the computer connected to the machine and then pressing run to begin the test. The system recorded the force that applied during the test until the bond strength fails to keep the rebar within the concrete

cylinder. The recorded maximum force (F_{max}) is the force that required breaking down the bonds. Then the maximum force is divided by the contact area ($A_{contact}$) between the rebar and concrete to get the maximum allowable shear stress (τ_{max}) using the following equations:

$$\tau_{max}\,(kPa) = \frac{F_{max}\ (kN)}{A\ contact\ \ (m^2)} \tag{10}$$

$$A_{contact}\ \ = D\ \pi\ L_{contact} \tag{11}$$

Where D is the rebar diameter = 0.0127 m, $L_{contact}$ is the length of rebar that is in contact with the concrete = 0.0762 m and $A_{contact}$ = 0.003039 m^2.

CHAPTER IV

Results and Discussion

4.1 Introduction

In this chapter, the experimental results that were obtained by three sets of experiments are discussed. The experiments were carried out to investigate the effect of different pH and salinity on the corrosion rate of reinforced concrete, on the bond behavior between the steel rebar and the concrete element, and on the steel rebar physical properties. The first experiment results investigated the relation between the corrosion rate vs. different pH and salt concentration for both uncoated and zinc coated steel rebar. The second experiment tested the bond behavior between the steel rebar and the concrete element to investigate the maximum force and shear stress required to cause failure to these bonds for both uncoated and coated steel rebar embedded in concrete elements, and the last experiment focused on the physical properties of the steel rebar represented by Rockwell hardness, Vickers hardness, yield strength, and tensile strength.

4.2 Corrosion rate of reinforced concrete

In this study, two methods were used to measure the corrosion rate of steel rebar; the first one was Tafel test method, and the second one was the weight loss method.

4.2.1 Tafel Test method

The corrosion tester results that represented by both corrosion current and corrosion rate of steel rebar samples submersed in solutions of different pH and NaCl concentration as corrosive environments are shown in table 4.1.

Table 4.1 Corrosion tester results of corrosion current and corrosion rate for related samples submersed in solutions of different pH and NaCl concentration

Sample No	pH Value for the submersion solution	Corrosion current (I_{corr})	Corrosion rate (mpy)
1	2	32.727 μA	15.066
2	4	18.345 mA	8455.4
3	7	451.261 μA	207.74
4	10	7.106 μA	3.2715
5	12	42.855 nA	0.019729
	NaCl Concentration for the submersion solution (g/L)		
6	3	16.996 nA	0.0078242
7	6	251.486 μA	115.77
8	9	10.252 nA	0.0047197
9	`12	0 A	$2.4811*10^{-32}$
10	15	167.715 mA	77208

- mA: Milliampere, μA :Microampere, nA: Nanoampere
- (mpy) milli-inches per year

The Tafel plots for the steel rebar circular samples that were subjected to different range of pH and salinity are shown below:

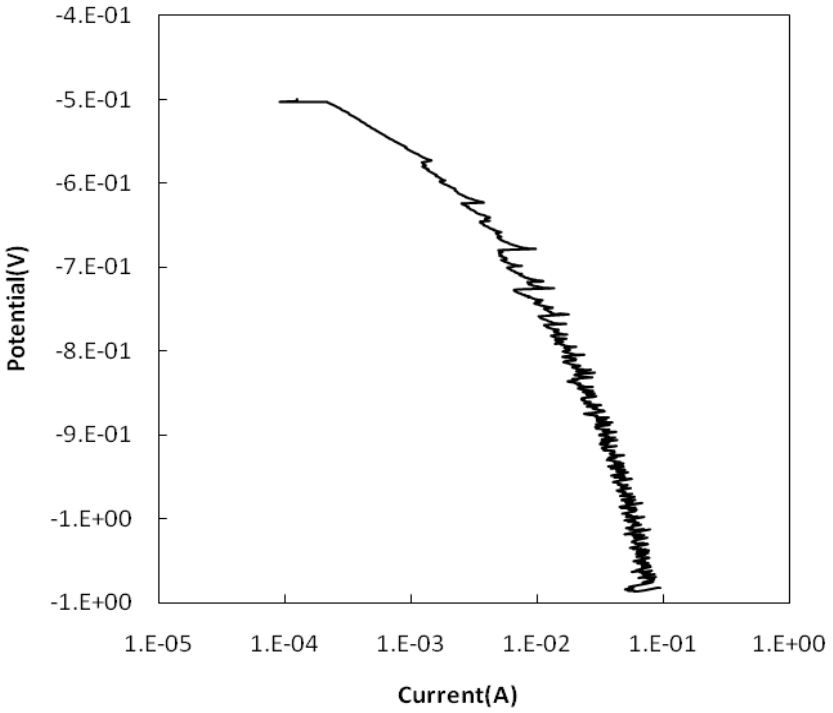

Figure 4.1 Tafel plot for steel rebar sample at pH=2

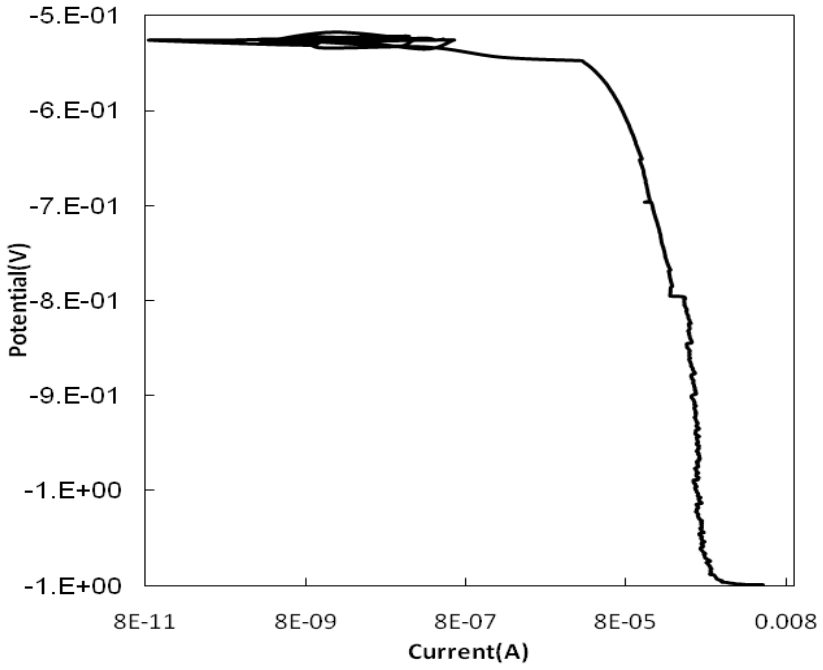

Figure 4.2 Tafel plot for steel rebar sample at pH=4

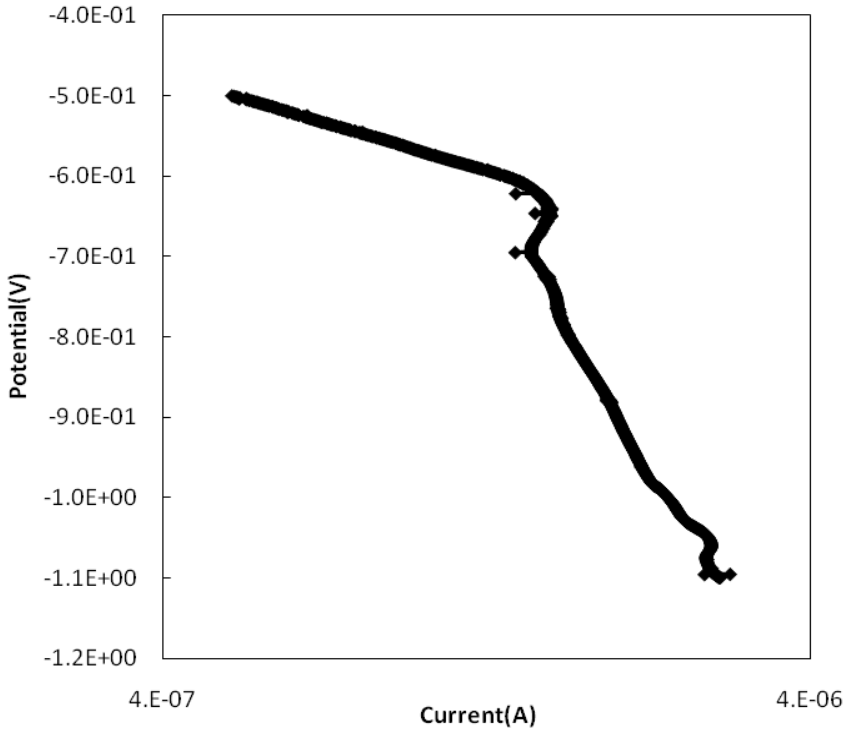

Figure 4.3 Tafel plot for steel rebar sample at pH= 7

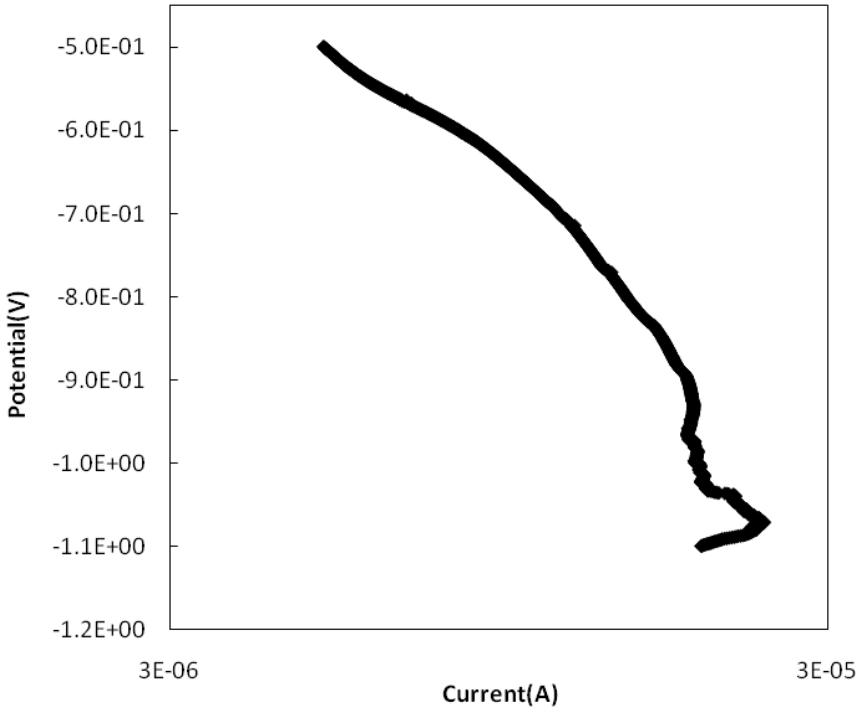

Figure 4.4 Tafel plot for steel rebar sample at pH=10

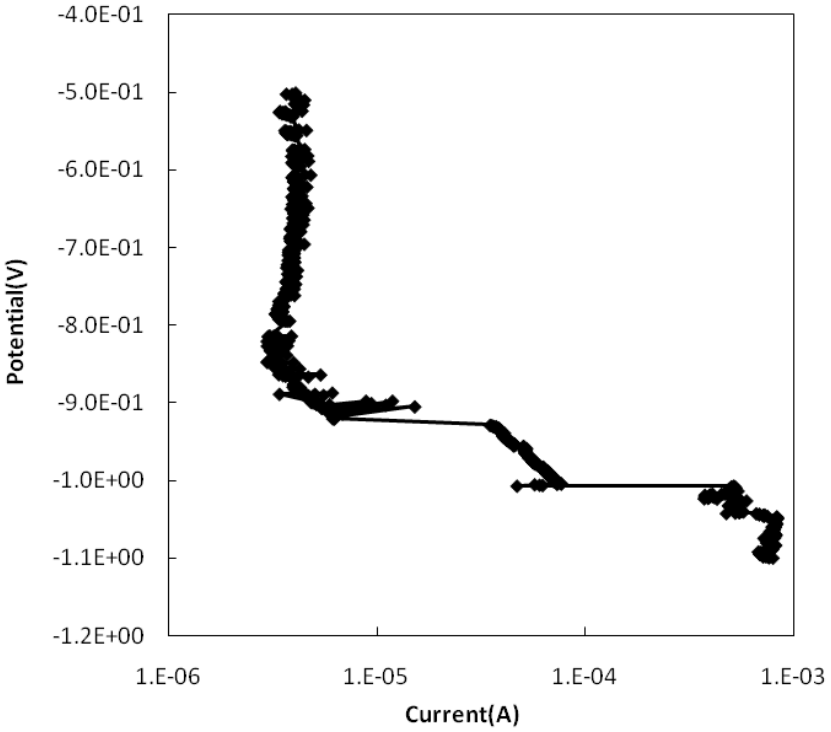

Figure4.5 Tafel plot for steel rebar sample at pH=12

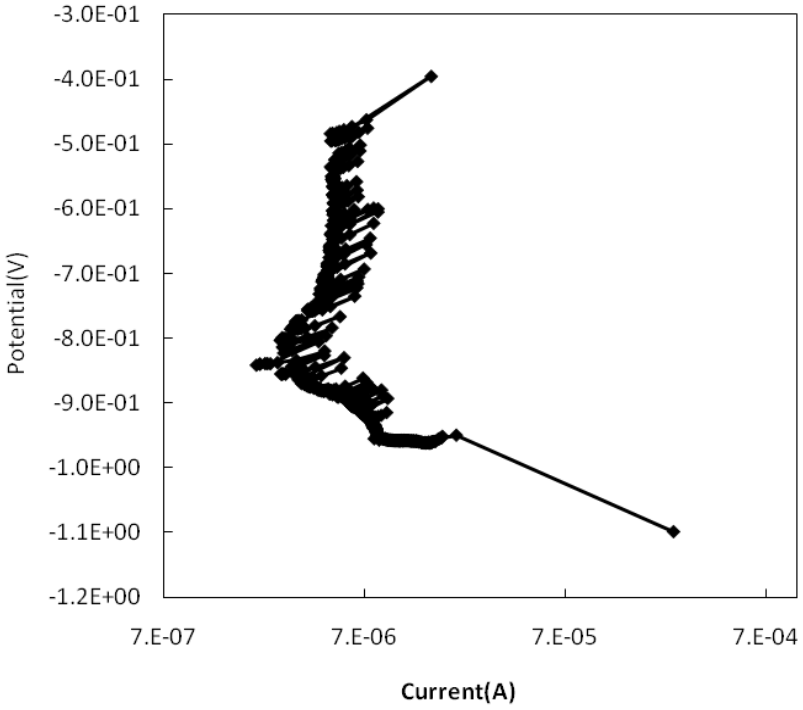

Figure 4.6 Tafel plot for steel rebar sample of salt (NaCl) concentration = 3 g/l

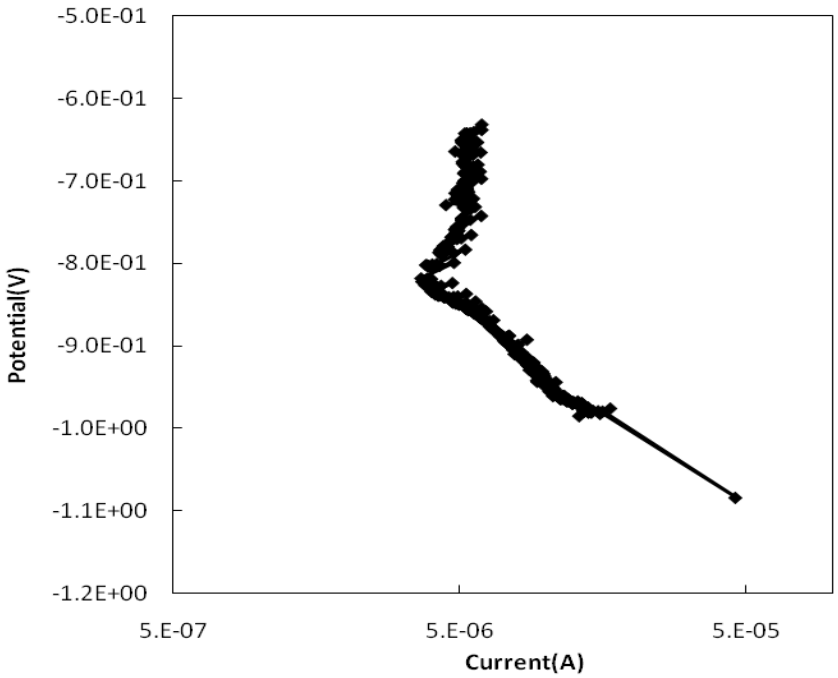

Figure 4.7 Tafel plot for steel rebar sample of salt (NaCl) concentration = 6 g/l

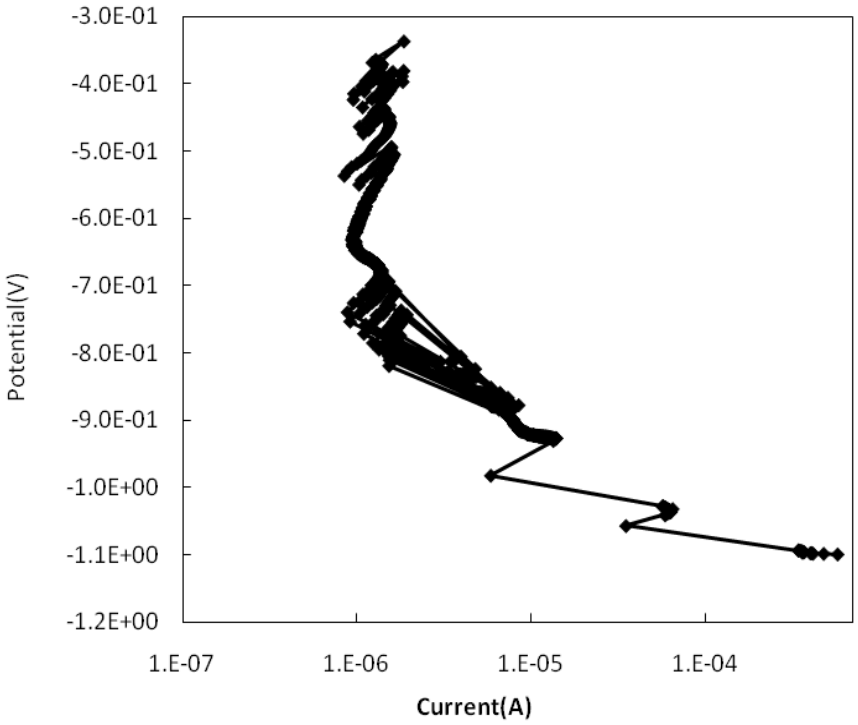

Figure 4.8 Tafel plot for steel rebar sample of salt (NaCl) concentration = 9 g/l

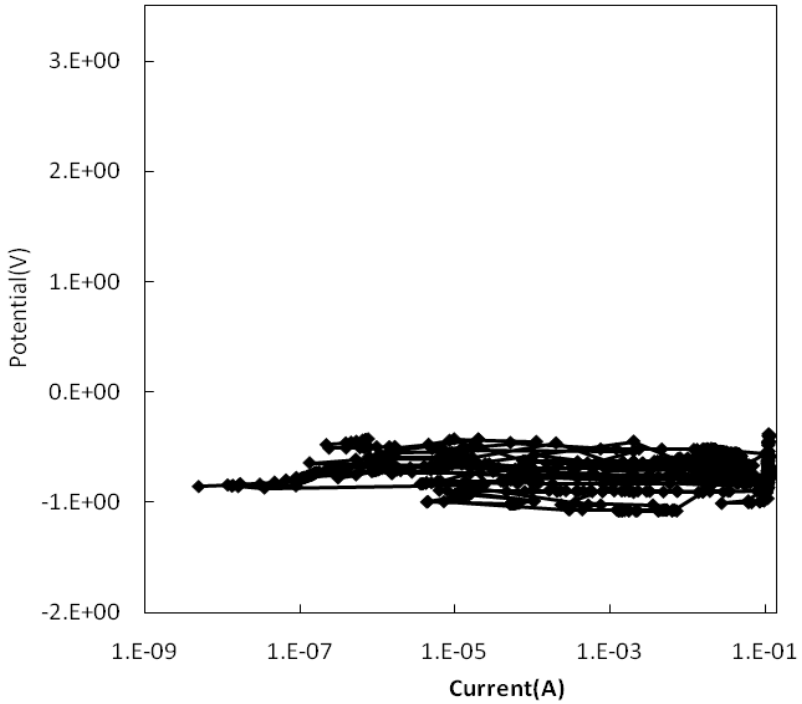

Figure 4.9 Tafel plot for steel rebar sample of salt (NaCl) concentration = 12 g/l

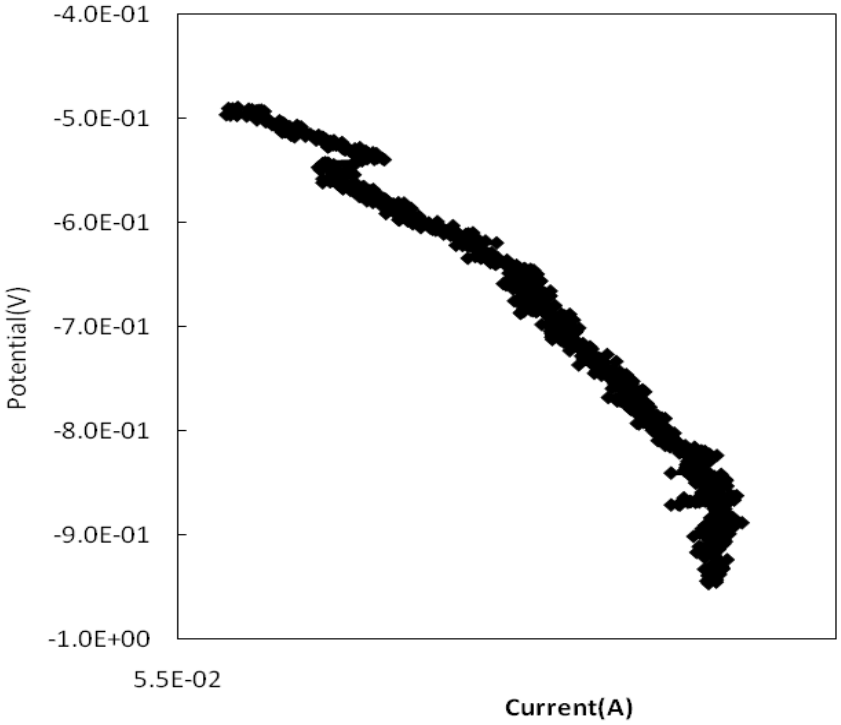

Figure 4.10 Tafel plot for steel rebar sample of salt (NaCl) concentration = 15 g/l

The corrosion rate relations vs. different pH and salt concentration are shown in figures 4.11 and 4.12. The result obtained by using solution with pH= 2 has been ignored because it was not reasonable and that is due to the limitation of acidity that the corrosion tester equipment can deal with. The increase of salt concentration in the solution (15 g/l NaCl) led to breakdown or destruction of the passive layer which then led to a sharp increase in the corrosion rate (77208 mpy). This result is included in table 4.1 but did not appear in Fig. 4.12 because it makes the other points unrecognizable.

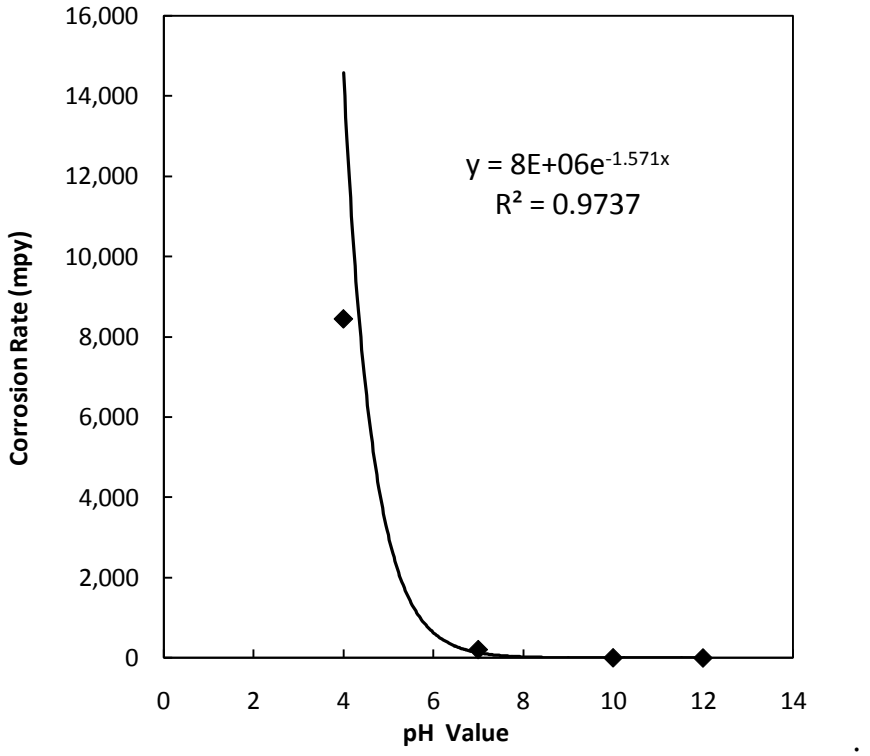

Figure 4.11 Corrosion rate vs. pH for circular samples of steel rebar

In figure 4.11, the corrosion rate increased when the acidity of the submersion solutions was increased due to the hydrogen evolution, so when the HCl concentration increases, the corrosion current density ($I_{corr.}$) increases. The corrosion rate decreased with the decrease in acid concentration. At the range of pH from 7-10, the corrosion

decreased. On the other hand, the corrosion rate decreased with increasing NaOH concentration in the solutions due to the formation of a passive layer of ferrous hydroxide [$Fe(OH)_2$] which is insoluble in water and acts as a barrier layer that isolate the metal from its environment. As the concentration of alkaline increases, the passive layer converts to a thicker layer of ferric hydroxide [$Fe(OH)_3$], i.e. rust, which is also insoluble in water and isolates the metal from its environment, thus decreases the corrosion rate of the metal.

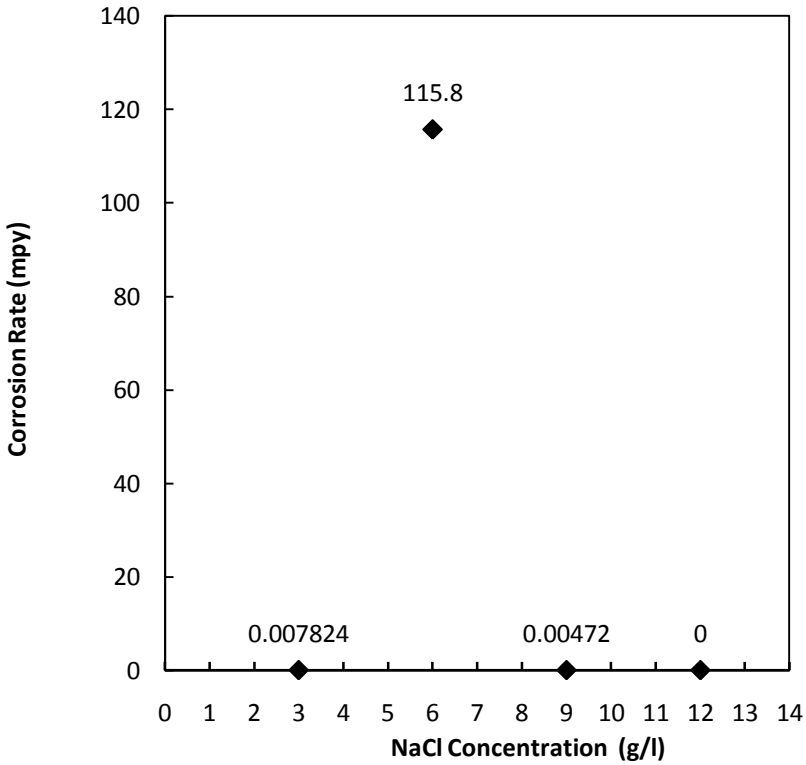

Figure 4.12 Corrosion rate vs. salt (NaCl) concentration for circular samples of steel rebar

In figure 4.12, the increase in the corrosion rate was observed as a result of an increase in the salinity of the submersion solution. This is due to the increase of corrosion current density (I_{corr}.) when the salt concentration increases,. Between the ranges of 3-6 g/l of salt concentration, the corrosion rate increases, but after the saturation

point, there is not enough oxygen for the metal corrosion which leads to decrease the corrosion rate.

4.2.2 Weight loss method

This experiment is designed to investigate the corrosion rate of (uncoated and zinc coated) steel rebar specimens embedded in cylindrical concrete element samples. These samples were made thin and porous; they had a diameter of 1.0 inch. To increase the porosity of the concrete element, 1 ml of air intranet (AE 90) was added, and the water content was increased in the concrete mixture. The experiment was carried out to determine the relation between the corrosion rate and pH of the surrounding medium (pH range = 1-14), and also the relation between the corrosion rate and the salinity of the surrounding medium for both uncoated and zinc coated reinforcement steel rebar.

The zinc coating process was done three times for each steel rebar by using professional cold galvanizing compound zinc spray depending on the company instruction of this product which mentioned that the coating should be two times or more. Four images were taken for uncoated rebar and for each layer of the coating process by using scanning electron microscope (SEM). The results of the images showed that the zinc coating was as particles of zinc which had porous in between.

The four images of uncoated and three layers zinc coated steel rebar are shown in figure 4.13 a, b, c, and d respectively.

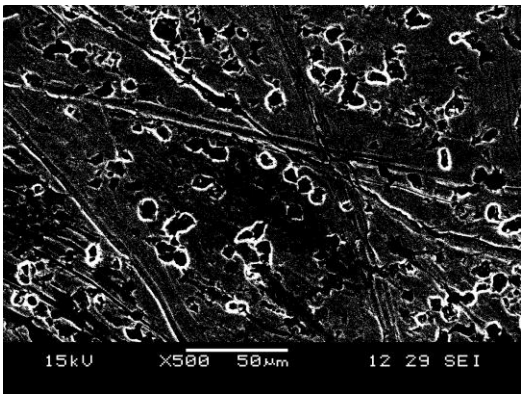

(a) Uncoated steel

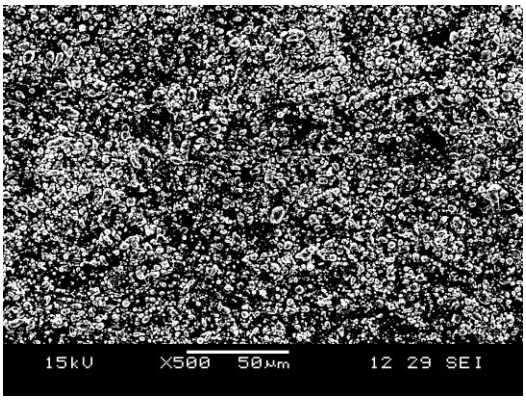

(b) One layer zinc coated

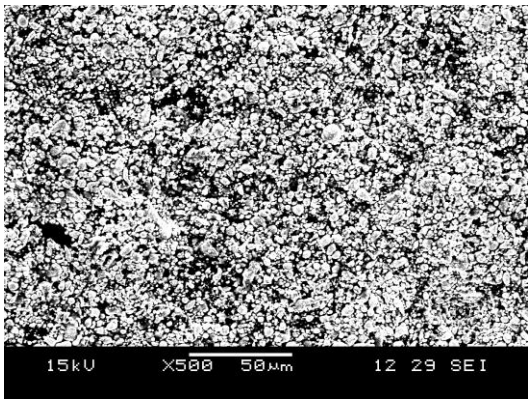

(c) Two layer zinc coated

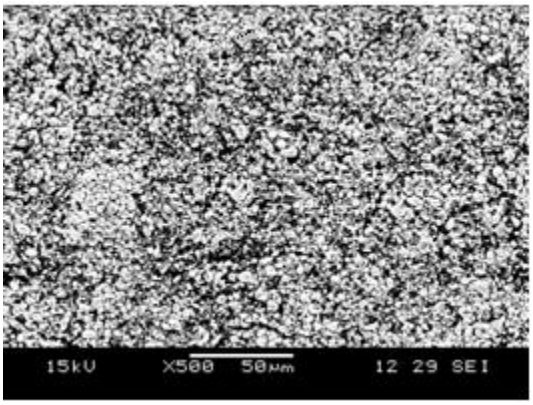

(d) Three layer zinc coated

Figure 4.13 Four images of uncoated and three layers zinc coated steel rebar

The calculated corrosion rate for the uncoated and zinc coated rebar of the samples are shown in tables 4.2 and 4.3 respectively.

Table 4.2 Corrosion rate of the fifteen uncoated rebar samples after 3 months

Sample no.	pH Value for the submersion solution	W1 g/ 1 inch length	W2 g/ 1 inch length	W (weight loss) g/ 1 inch length	Rate of corrosion (µm/year)
1	1.5	24.525	22.26	2.265	930.14
2	2.1	24.5	22.57	1.93	792.57
3	2.6	24.725	23.22	1.505	618.04
4	3.2	24.6	23.65	0.95	390.12
5	4.3	24.55	24.3	0.25	102.66
6	7.2	24.425	24.35	0.075	30.80
7	10.3	24.3	24.25	0.05	20.53
8	11.5	24.45	24.41	0.04	16.43
9	12.8	24.425	24.4	0.025	10.27
10	13.9	24.55	24.53	0.02	8.21
	NaCl Concentration in the submersion solution g/L				
11	10	23.575	23.49	0.085	34.91
12	20	24.325	24.21	0.115	47.23
13	30	24.2	24.03	0.17	69.81
14	40	24.725	24.53	0.195	80.08
15	50	24.7	24.68	0.02	8.21

Table 4.3 Corrosion rate of the fifteen coated rebar samples after 3 months

sample no.	pH Value for the submersion solution	W1 g/ 1 inch length	W2 g/ 1 inch length	W (weight loss) g/ 1 inch length	Rate of corrosion (µm/year)
1	1.5	25.11	23.131	1.979	812.75
2	2.1	25.49	23.972	1.518	623.35
3	2.6	24.82	23.760	1.060	435.35
4	3.2	24.81	24.227	0.583	239.22
5	4.3	24.81	24.664	0.146	59.79
6	7.2	24.93	24.891	0.039	16.15
7	10.3	25.66	25.636	0.024	10.00
8	11.5	25.37	25.352	0.018	7.20
9	12.8	25.21	25.200	0.010	4.25
10	13.9	24.62	24.608	0.012	4.76
	NaCl Concentration in the submersion solution g/L				
11	10	24.85	24.823	0.027	10.93
12	20	25.23	25.188	0.042	17.32
13	30	24.16	24.097	0.063	25.83
14	40	25.44	25.359	0.081	33.07
15	50	24.72	24.711	0.009	3.75

- (µm/year) is micro meter per year.

Figures 4.14 and 4.15 represent table 4.2 , and figures 4.16 and 4.17 represent table 4.3 which are shown below:

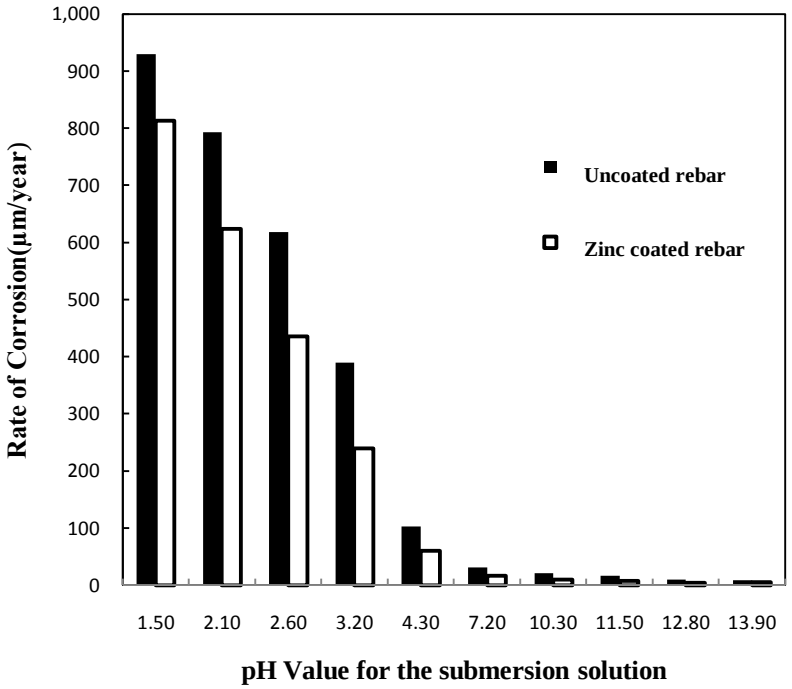

Figure 4.14 Corrosion rate vs. pH for the submerged solution

The corrosion rate of the rebar increased when the acidity of the submersion solutions was increased, due to the evolution of hydrogen gas which needed more dissolution of the metal. The corrosion rate decreased when the alkalinity was increased until it reached the smallest value at pH= 13.9 (which is 8.21 µm/year for uncoated and 4.76 µm/year for coated rebar). The corrosion rate decreased because of the formation of a passive layer, which is a layer of iron hydroxide called rust has the composition $Fe(OH)_3$ and is formed with the increase in alkalinity of the solution in which the steel rebar was immersed. This layer is insoluble in water which limits the diffusion of oxygen and causes the decrease in the corrosion rate.

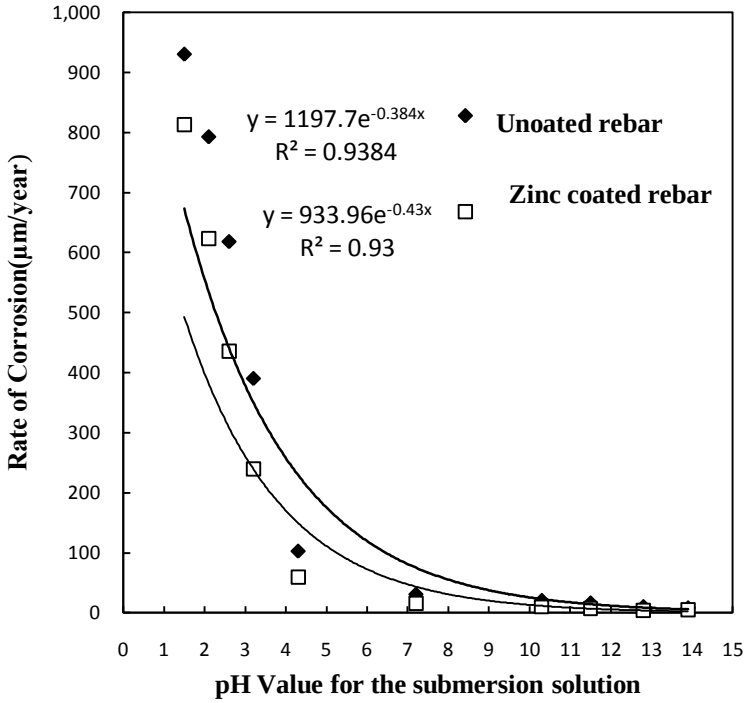

Figure 4.15 Correlation between corrosion rate and pH

The best fitting curve that correlates the corrosion rate with pH (pH range =1-14) is the exponential equation with a coefficient of R2 = 0.9384, 0.93 for uncoated and coated rebar respectively.

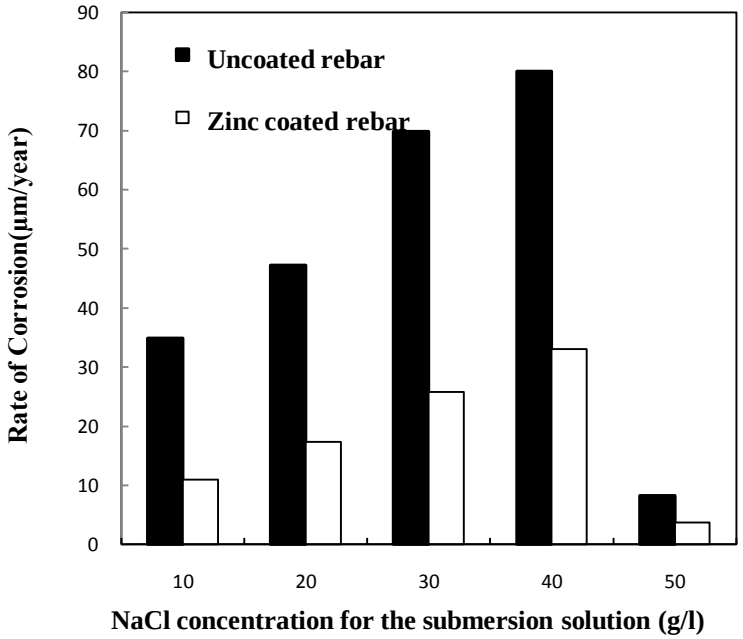

Figure 4.16 Corrosion rate vs. salt (NaCl) concentration for the submerged solution

In figure 4.16, the rebar corrosion rate increased with the increase in the salinity of the submersion solutions until reach the value 80.08 µm/year for uncoated rebar and 33.07 µm/year for coated rebar. Then, the corrosion rate decreased with an increase in the concentration of the salt due to a decrease of the dissolved oxygen in the solution.

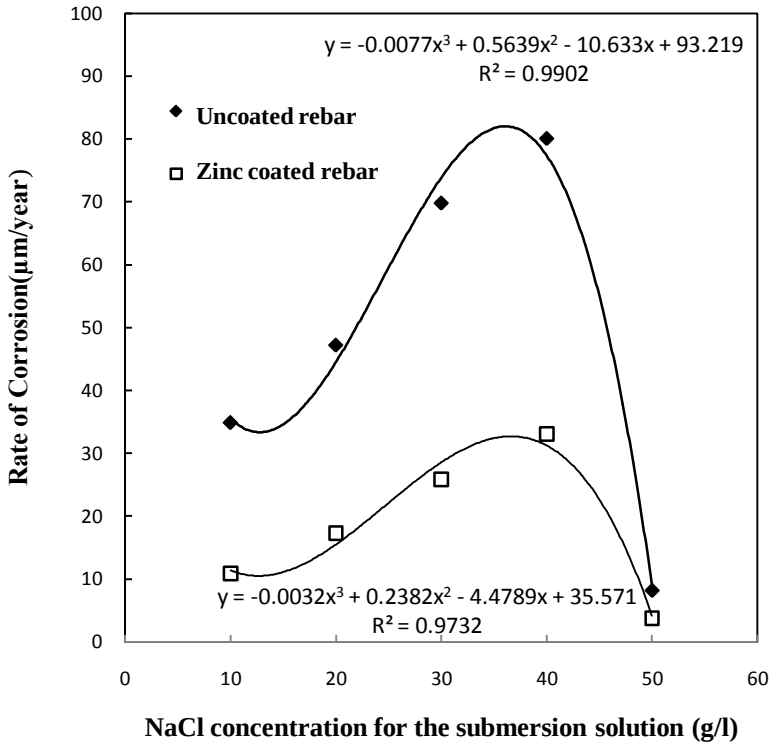

Figure 4.17 Correlation between corrosion rate and (NaCl) concentration

The best fitting curve that correlates the corrosion rate with the salinity of the submersion solutions is a third degree polynomial equation with a coefficient of R^2 = 0.99, 0.9732 for uncoated and coated rebar respectively.

4.3 Bond strength test

This experiment is designed to determine the relation between the pH (pH range = 1-14) and salinity of the surrounding medium with the maximum allowable shear stress required to cause bond strength failure between the concrete and reinforcement steel.

Table 4.4 Maximum allowable shear stress required to cause failure during bond strength test of the uncoated rebar concrete samples after 3 months

Sample No.	pH for the submersion solution	Max Force (F_{max}) (kip)	Max Force (F_{max}) (kN)	Max shear stress (τ_{max}) (kPa)
1	1.5	0.88	3.91	1288.19
2	2.1	0.94	4.18	1376.02
3	2.6	1.2	5.34	1756.62
4	3.2	1.3	5.78	1903.01
5	4.3	1.4	6.23	2049.39
6	7.2	1.46	6.49	2137.22
7	10.3	1.78	7.92	2605.66
8	11.5	2.1	9.34	3074.09
9	12.8	2.23	9.92	3264.39
10	13.9	2.61	11.61	3820.66
	NaCl Concentration in the submersion solution g/L			
11	10	3.3	14.68	4830.72
12	20	2.38	10.59	3483.97
13	30	2.1	9.34	3074.09
14	40	0.99	4.40	1449.21
15	50	1.92	8.54	2810.60

- (Kip) kilo pound, (KN) kilo Newton, and (KPa) kilo Pascal.

Table 4.5 Maximum allowable shear stress required to cause failure during bond strength test of the zinc coated rebar concrete samples after 3 months

Sample No.	pH for the submersion solution	Max Force (F_{max}) (kip)	Max Force (F_{max}) (kN)	Max shear stress (τ_{max}) (kPa)
16	1.5	1.22	5.43	1785.90
17	2.1	1.37	6.09	2005.48
18	2.6	1.42	6.32	2078.67
19	3.2	1.55	6.9	2268.98
20	4.3	1.58	7.03	2312.89
21	7.2	1.61	7.16	2356.81
22	10.3	1.74	7.74	2547.11
23	11.5	1.96	8.72	2869.16
24	12.8	2.04	9.07	2986.26
25	13.9	2.12	9.43	3103.37
	NaCl Concentration in the submersion solution (g/L)			
26	10	2.9	12.9	4245.18
27	20	2.02	8.99	2956.99
28	30	1.82	8.10	2664.22
29	40	1.5	6.67	2195.78
30	50	1.81	8.05	2649.58

The bond strength test showed that the force required to pull out the embedded rebar from the concrete elements increased with the increase in pH for immersing solution; such behavior could be related to the decrease of the corrosion rate with the increase of the pH of the immersing solution.

The bond strength test showed that the force required to pull out the embedded rebar from the concrete elements decreased with the increase in the salinity of the immersing solution. This behavior could be related to the increase of the corrosion rate with the increase of the salinity of the immersing solution.

Figures 4.18 and 4.19 represent tables' 4.4 and 4.5 results graphically:

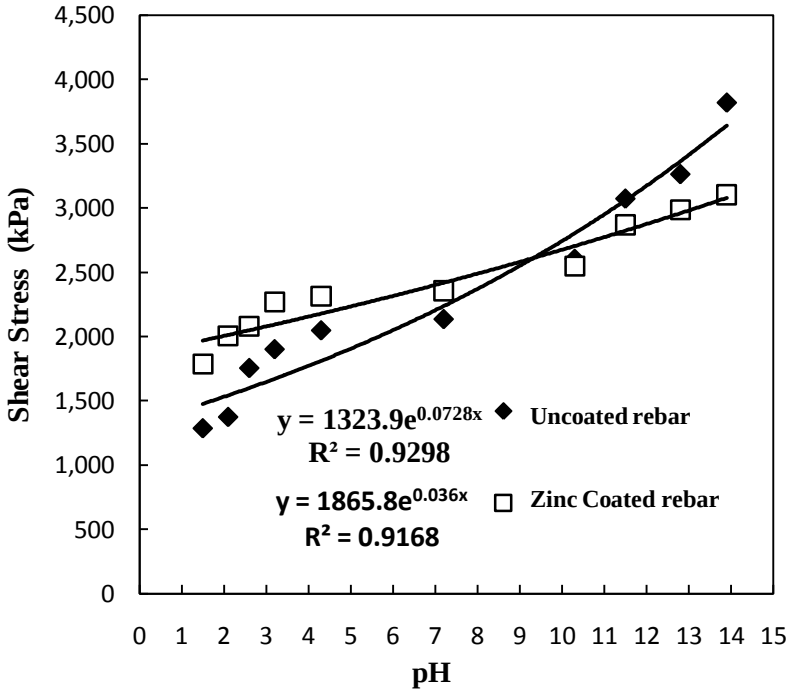

Figure 4.18 Correlation between the maximum allowable shear stress vs. pH of the submersion solution

From Figure 4.18, it can be noticed that the shear stress required to pull out the embedded zinc coated rebar is greater than that of the uncoated rebar. This is due to the positive effect of the coating process in decreasing the corrosion rate. However for pH ≈ > 9.3, the shear stress for uncoated rebar seems to be greater than that of the zinc coated rebar. This is attributed to two conjugated reasons: the first reason is the decrease of the corrosion rate due to the increase of pH, and the second is the smoothing effect of zinc

coating. The best fitting curve that correlates the shear stress with pH (pH range =1-14) is an exponential equation with a coefficient of R^2 = 0.9298, 0.9168 for uncoated and zinc coated rebar respectively.

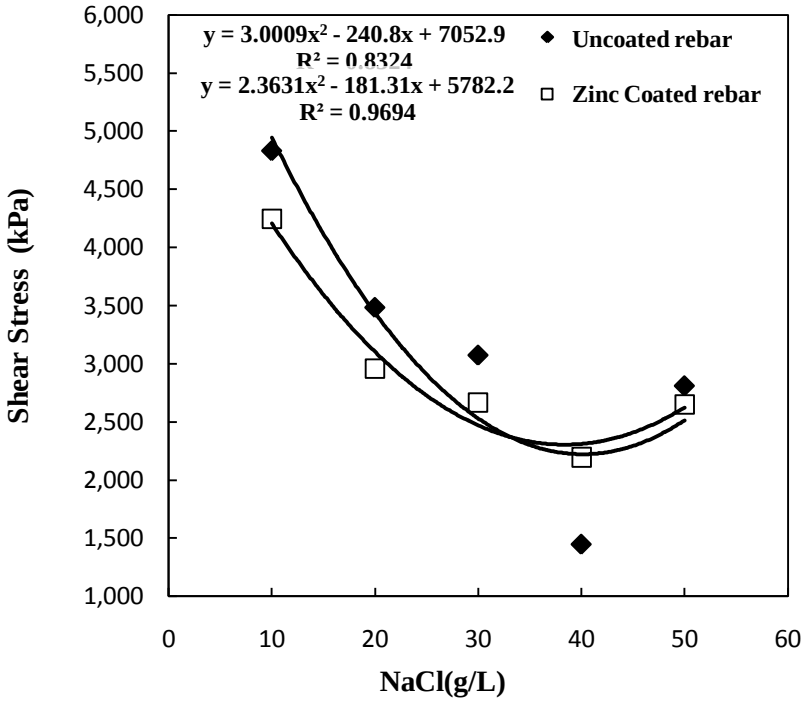

Figure 4.19 Correlation between the maximum allowable shear stress vs. NaCl concentrations of the submersion solution

It can be noticed from figure 4.19 that the shear stress required to pull out embedded zinc coated rebar is less than that of uncoated rebar for the salinity 10 ~ 32 g/l (NaCl) of the immersing solution. This may be attributed to two conjugated reasons: the first reason is the decrease of the corrosion rate due to the decrease of salinity, and the second is the smoothing effect due to zinc coating. However, when corrosion rate increases due to an increase in salinity (for salinity concentration > 32 g/l), the shear stress for zinc coated rebar seems to be greater than that of uncoated rebar due to the positive effect of zinc coating in decreasing the corrosion rate. The best fitting curve that

correlates the shear stress with the salinity of the submersion solutions is a second degree polynomial equation with a coefficient of R^2 = 0.8324, 0.9694 for uncoated and for zinc coated rebar respectively.

4.4 Physical properties of the steel rebar

This experiment is designed to investigate the hardness, yield strength, and tensile strength of steel rebar specimens embedded in cylindrical concrete elements which were immersed in solutions of different pH and salt concentration, and the effect of corrosion rate on the physical properties of reinforcing rebar.

Based on the observation of the steel surface, the eye inspection for corrosion in the imbedded portion of the steel rebar comparing with the exposed portion was almost negligible. Most of the corrosion was in the exposed part of the steel rebar which was exposed to the corrosion solutions.

4.4.1 Rockwell hardness

The clean and rusted steel rebar was subjected to Rockwell hardness test. The Rockwell hardness value for clean steel rebar was 20.6 kg / mm^2. The tensile strength for clean steel rebar was 90.4 ksi.

Table 4.6 represents the results of the Rockwell hardness test as well as the tensile strength for rusted steel rebar.

Figures 4.20 and 4.21 show the relation between the corrosion rate of steel rebar vs. the Rockwell hardness and the tensile strength respectively.

Table 4.6 Rockwell hardness and Tensile strength of the rusted rebar vs. pH and NaCl concentration of the submersion solution

Sample no.	pH Value for the submersion solution	HRC 1	HRC 2	HRC 3	HRC 4	HRC 5	Ava. HRC (kg/mm^2)	Tensile Strength (Ksi)
1	4	18.6	18.2	27	28.7	25.5	23.6	120.8
2	6.7	15.9	10	13.8	13.1	9.6	12.5	96
3	10	18.1	27.4	10.1	19.2	5.9	16.14	101.42
4	12	20.9	19.9	20.4	26.1	15.2	20.5	111.5
5	14	19.6	22.4	21.2	23	17.8	22.6	117.8
	NaCl Concentration in the submersion solution (g/L)							
6	3	10.4	12.7	12.5	14.6	12.3	12.5	96
7	6	11.8	22.9	14.7	7.9	16.9	14.84	98.84
8	9	13.9	13.8	15.9	12.7	18.7	15	99
9	12	16.1	15.5	10.2	18.4	18.6	15.8	100.6
10	15	23.9	19.1	23.4	20.9	26.4	22.74	118.22

- (Ksi) is kilo pound per square inch.

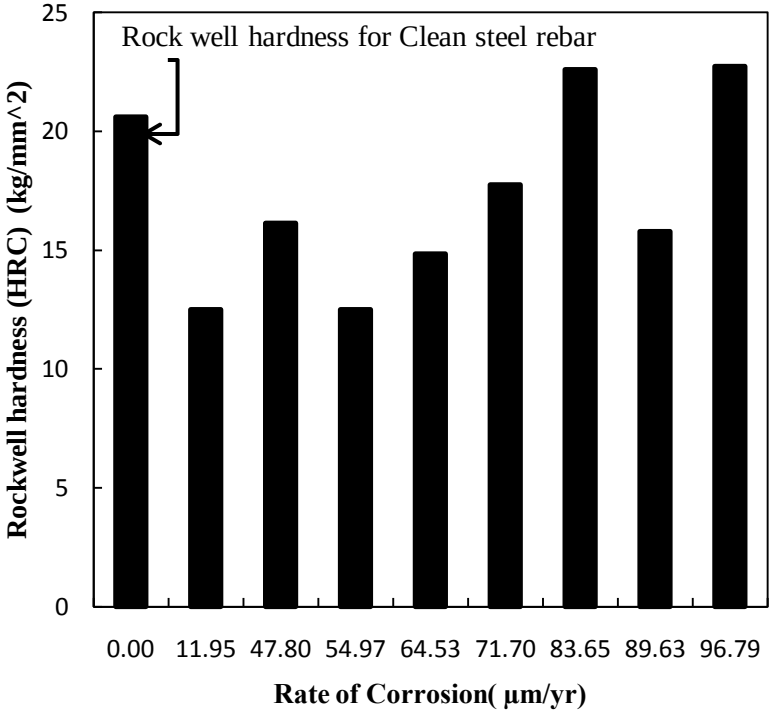

Figure 4.20 Rockwell hardness vs. corrosion rate for clean and rusted steel rebar

From figure 4.20, the average Rockwell hardness for rusted steel rebar (17.62 kg/mm^2) was found to be almost less than that for cleaned rebar (20.6 kg/mm^2).

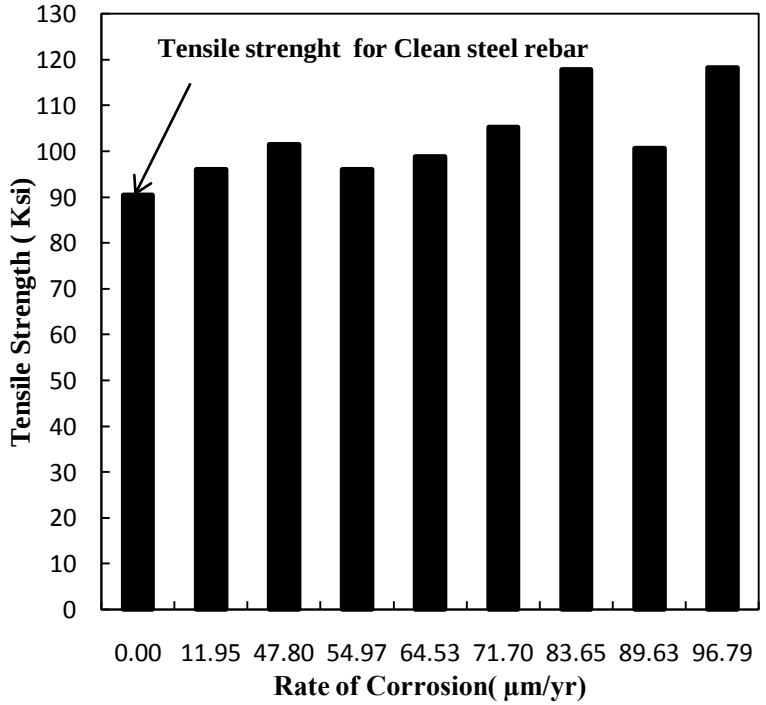

Figure 4.21 Tensile strength vs. corrosion rate for clean and rusted steel rebar

Rusted rebar show a tendency of increase in tensile strength values in comparing with the clean rebar. The tensile strength average value for rusted rebar was found to be 104.26 ksi and for clean rebar was 90.4 ksi. However, this increase in tensile strength values are not related to increase in corrosion rate, but the tensile strength values that are provided by conversion chart are approximate.

4.4.2 Vickers Hardness

The clean and rusted steel rebar was subjected to Vickers hardness test. The Vickers hardness value for clean steel rebar was 264 kg / mm^2, and the yield strength for clean steel rebar was 88 ksi. The following table and figures show the results of the Vickers hardness and the yield strength for rusted steel rebar.

Table 4.7 represents the results of the Vickers hardness test as well as the calculated yield strength for rusted steel rebar.

Figures 4.22 and 4.23 show the relation between the corrosion rate of steel rebar vs. the Vickers hardness and the yield strength respectively.

Table 4.7 Vickers hardness and yield strength of the rusted rebar vs. pH and Nacl concentration of the submersion solution

sample no.	pH Value for the submersion solution	HV 1	HV 2	HV 3	HV 4	HV 5	HV av. (kg/mm^2)	Yield Strength (Ksi)
1	4	250	310	280	270	290	280	93.3
2	6.7	250	300	283	256	301	278	92.7
3	10	201	259	274	260	248	248.4	82.8
4	12	265	275	281	262	274	271.4	90.5
5	14	267	253	244	277	266	261.4	87
	NaCl Concentration in the submersion solution (g/L)							
6	3	272	289	286	285	280	282.4	94.1
7	6	239	265	233	280	243	252	84
8	9	270	245	255	240	290	260	86.7
9	12	254	280	265	278	270	269.4	89.8
10	15	300	250	270	260	295	275	91.7

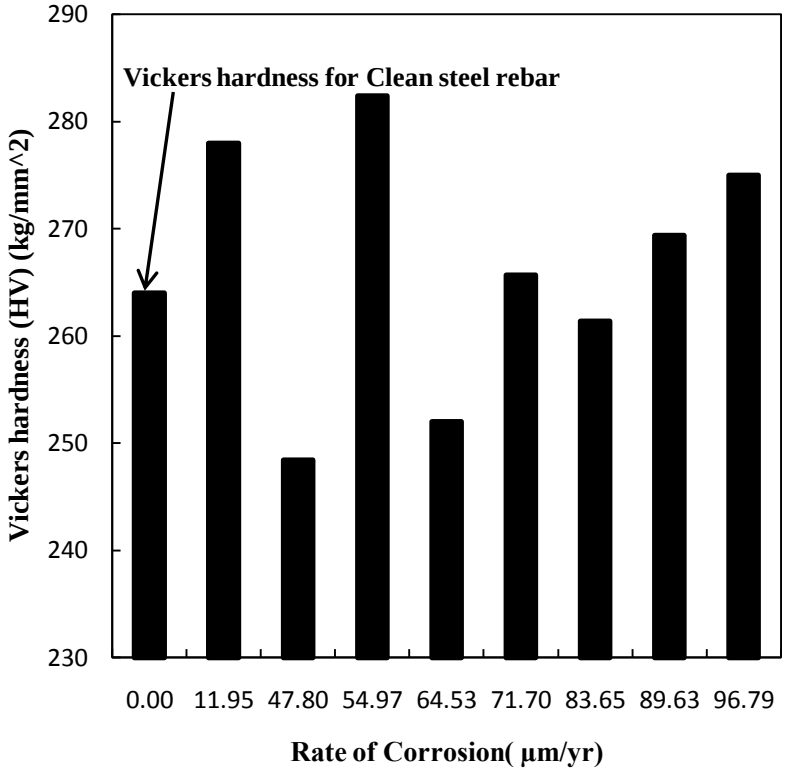

Figure 4.22 Vickers hardness vs. corrosion rate for clean and rusted steel rebar

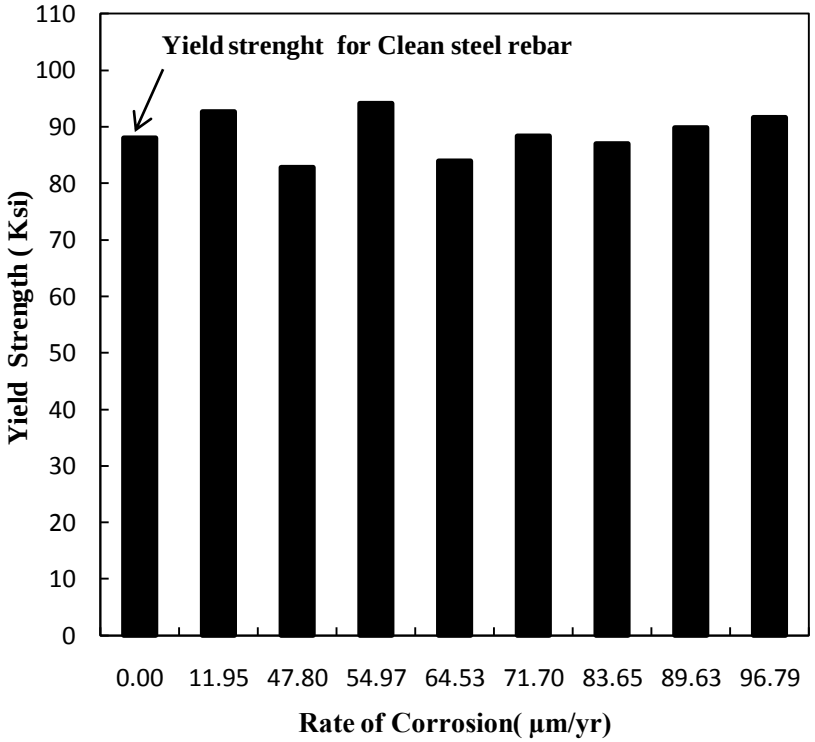

Figure 4.23 Yield strength vs. corrosion rate for clean and rusted steel rebar

From figure 4.22, Vickers hardness test for the rusted rebar did not show a noticeable difference in the hardness value from that of the clean rebar, since the corrosion does not affect the carbon layers of the steel rebar composition which accounts for its hardness. Vickers hardness average value for rusted rebar was 266.5 kg / mm^2 and for clean rebar was 264 kg / mm^2.

In figure 4.23, even though the yield strength values for the rusted rebar did not show a noticeable difference from that of the clean rebar, the average value for rusted rebar was found to be 88.8 ksi and for clean rebar was 88 ksi, so they are almost the same.

CHAPTER V

Conclusion and Recommendations

5.1 Conclusion

This study focused on the effect of pH and salinity on the corrosion rate of reinforced concrete and on how this corrosion affects the bond strength between the concrete and uncoated or cold-galvanized steel rebar. The physical properties: Rockwell hardness, Vickers hardness, tensile strength, and yield strength were measured and related to the corrosion rate at controlled variables of pH and salinity. The following are the conclusions and recommendations based on the results of these experiments.

5.1.1 Corrosion rate of reinforced concrete

The corrosion rate experimental results indicate the following:

i. The Tafel test results illustrated that the corrosion rate is inversely proportional to pH solution. Also, the corrosion rate is proportional to salt concentration.

ii. The weight loss method confirmed the results of the Tafel test.

iii. The coating process images stated that the cold galvanizing zinc spray coating was as particles of zinc not a film layer of zinc.

iv. The cold-galvanized steel rebar showed superior corrosion resistance to bare rebar (i.e., lower corrosion rate) across the pH and salinity range probed.

5.1.2 Bond strength test

The bond strength test results indicate the following conclusions:

i. Bond strength between the rebar and the concrete as measured by pull out strength, was proportional to pH.

ii. The lower corrosion observed for cold-galvanized steel rebar resulted in superior pull out strength compared to bare steel rebar across the pH range probed.

iii. Bond strength between the steel rebar and the concrete as measured by pull out strength, was inversely proportional to salinity.

iv. The pull out strength was lowered for cold-galvanized rebar at salt concentration below 32 g/l compared to bare rebar. For higher salt concentration, the cold-galvanized rebar displayed higher pull-out strength.

v. It can be concluded that the corrosion rate of the embedded rebar in reinforced concrete affects their structural performance in two ways, either by reducing their cross-section area or by deteriorating the strength of the bonds between the steel and the concrete.

5.1.3 Physical properties of the steel rebar

According to the results obtained, the following conclusions can be drawn:

i. The rate of corrosion in the imbedded portion of the steel rebar was negligible in comparison with the exposed portion of steel which was exposed to the corrosive environment.

ii. The Rockwell hardness value for the rusted rebar was less than that for the clean rebar, as the Rockwell hardness decreased for rusted areas.

iii. The Vickers hardness value for the rusted rebar did not show a noticeable difference with that for the clean rebar, and the logical reason for this is that the corrosion rate did not affect the carbon layers of steel rebar composition which support its hardness.

iv. The Yield strength for the rusted rebar did not show a noticeable difference with that for the clean rebar while the tensile strength for the rusted rebar showed a little increase in comparison with the clean rebar. In general, the corrosion rate had no noticeable effect on the steel rebar physical properties.

5.2 Recommendations

The future recommendations for the work are as follows:

i. Investigate the effect of applying more than three layers of the cold-galvanizing zinc coating on the corrosion rate of reinforced concrete and the bond strength between the concrete and the steel rebar.

ii. Repeat the conducted experiments in this study using epoxy coating as a protection method for the rebar instead of cold-galvanizing zinc coating, and compare the results.

iii. Evaluate the interfacial strength effect which results from using various rebar coating methods on bond strength between the concrete and the steel rebar.

iv. Investigate the effect of the corrosion product volume on the bond strength of reinforced concrete across the pH and salinity range probed.

References

1. Associates, J. R. D. D., *Corrosion: Understanding the Basics*. ASM international 2000.
2. Robert G. Kelly, J. R. S., David W. Shoesmith, and Rudolph G. Buchheit, *Electrochemical Techniques in Corrosion Science and Engineering*. Marcel Dekker Inc: 2003; pp.1.
3. Perez, N., *Electrochemistry and corrosion science*. Kluwer Acadamic USA, 2004; pp.1-7.
4. Huang, Y.; Ji, D., Experimental study on seawater-pipeline internal corrosion monitoring system. *Sensors and Actuators B: Chemical* **2008,** *135* (1), 375-380.
5. Ibrahim, E. S., Corrosion control in electric power systems. *Electric Power Systems Research* **1999,** *52* (1), 9-17.
6. Tullmin,M.Corrosion-club.com. http://www.corrosion-club.com/basictheory.htm (accessed July 1, 2012), corrosion monitoring information.
7. Boulabiar, A.; Bouraoui, K.; Chastrette, M.; Abderrabba, M., A Historical Analysis of the Daniell Cell and Electrochemistry Teaching in French and Tunisian Textbooks. *Journal of Chemical Education* **2004,** *81* (5), 754-757.
8. National Research Council, *Review of the Bureau of Reclamation's Corrosion Prevention Standards for Ductile Iron Pipe*. National Academies Press: USA, 2009; pp.26.
9. Revie, R. W., *UHLIG'S CORROSION HANDBOOK*. Third ed.; John Wiley & Sons Inc: New Jersey 2011; pp.7.83.
10. Y Wang, Y. G. Z., W Ke, W H Sun, W L Hou, X C Chang, J Q Wang, Slurry erosion–corrosion behaviour of high-velocity oxy-fuel (HVOF) sprayed Fe-based amorphous metallic coatings for marine pump in sand-containing NaCl solutions. *Corrosion Science* **2011,** *53* (10), 3177-3185.

11. Lgried, M.; Liskiewicz, T.; Neville, A., Electrochemical investigation of corrosion and wear interactions under fretting conditions. *Wear* **2012,** *282–283*, 52-58.
12. Diomidis, N.; Mischler, S.; More, N. S.; Roy, M.; Paul, S. N., Fretting-corrosion behavior of β titanium alloys in simulated synovial fluid. *Wear* **2011,** *271* (7–8), 1093-1102.
13. Navid Rashidi, S. A.-S., Ramazan Asmatulu, Crevice Corrosion Theory, Mechanisms and Prevention Methods. In *Proceedings of the 3rd Annual GRASP Symposium*, Wichita State University, 2007; pp 215-216.
14. Chiu, S.-C. Surface Modification Processes and Fracture Behaviors of 7075-T6 Aerospace Al-Alloy. Ph.D. Thesis, Tatung University, July 2004.
15. You Lung, C.; Kuhl, T.; Israelachvili, J., Mechanism of cavitation damage in thin liquid films: Collapse damage vs. inception damage. *Wear* **1992,** *153* (1), 31-51.
16. Brandl, E.; Malke, R.; Beck, T.; Wanner, A.; Hack, T., Stress corrosion cracking and selective corrosion of copper-zinc alloys for the drinking water installation. *Materials and Corrosion* **2009,** *60* (4), 251-258.
17. Liang, P.; Li, X.; Du, C.; Chen, X., Stress corrosion cracking of X80 pipeline steel in simulated alkaline soil solution. *Materials & Design* **2009,** *30* (5), 1712-1717.
18. M. Z. Yang, a. J. L. L., a,* Q. Yang,a L. J. Qiao,a Z. Q. Qin,b and P. R. Nortonb, Effects of Hydrogen on Semiconductivity of Passive Films and Corrosion Behavior of 310 Stainless Steel. *Journal of the Electrochemical Society,* **1999,** *146* (6), 2107-2112.
19. Sanders, M. W. In Situ Small Scale Mechanical Characterization of Materials under Environmental Effects. Master Thesis, Texas A&M University, 2010.
20. R.Winston Revie , H. H. U., *Corrosion and corrosion control: an introduction to corrosion and engineering*. Fourth ed.; John Wiley & Sons Inc: Canada, 2008; pp. 53.5.95.
21. Ahmad, z., *Principles of Corrosion Engineering and Corrosion Control*. Elsevier Science & Technology Books: Great Britain, 2006; pp.3.
22. Schnepf, R., Iraq's Agriculture: Background and Status; Order Code RS21516; Congressional Research Service USA, 2003.

23. The Bottled Water Market in Iraq. United States Agency for International Development USA, 2007.
24. Luca Bertolini, B. E., Pietro Pedeferri, Rob P. Polder, *Corrosion of Steel in Concrete*. WILEY-VCH Verlag GmbH & Co. KGaA, Weinheim: 2004; pp.1.
25. C. M. Hansson; A. Poursaee, a. S. J. J. *CORROSION OF REINFORCING BARS IN CONCRETE*; Serial No. 3013; Skokie, Illinois, USA, 2007; pp 1-2.
26. Cabrera, J. G., Deterioration of Concrete due to Reinforcement Steel Corrosion. *Cement and Concrete Composites* **1996,** *18* (1), 47-59.
27. Ha-Won Song, V. S., Corrosion Monitoring of Reinforced Concrete Structures. *Int. J. Electrochem. Sci* **2007,** *2*, 1- 28.
28. Uhlig, H. H., Passivity in Metals and Alloys. *Corrosion Science* **1979,** *19* (11), 777-791.
29. Broomfield, J. P., *Corrosion of Steel in Concrete Understanding, Investigation and Repair*. E&FN Spon: London, 1997; pp.1-15.
30. Saetta, A. V.; Schrefler, B. A.; Vitaliani, R. V., The carbonation of concrete and the mechanism of moisture, heat and carbon dioxide flow through porous materials. *Cement and Concrete Research* **1993,** *23* (4), 761-772.
31. Kobayashi, K.; Takewaka, K., Experimental studies on epoxy coated reinforcing steel for corrosion protection. *The Journal of Cement Composites and Lightweight Concrete* **1984,** *6* (2), 99-116.
32. Hou, J.; Chung, D. D. L., Cathodic protection of steel reinforced concrete facilitated by using carbon fiber reinforced mortar or concrete. *Cement and Concrete Research* **1997,** *27* (5), 649-656.
33. Lindquist, W. D.; Darwin, D.; Browning, J.; Miller, G. G., Effect of Cracking on Chloride Content in Concrete Bridge Decks. *ACI MATERIALS JOURNAL* **2006,** *103* (6), 467-473.
34. Ragab, A.; Alawi, H.; Sorein, K., Effect of atmospheric and marine corrosive environments on tensile, impact and hardness properties of some steels. *Mechanics of Materials* **1994,** *18* (1), 69-77.
35. Tabor, D., *The Hardness and Strength of Metals*. Oxford University Press. New York, 1951; p p.1-18.

36. Boyle, B., A look at development in vapor phase corrosion inhibitors. *Metal Finishing* **2004,** *102* (5), 37-41.
37. Abdullah, A. Almusallam, Effect of degree of corrosion on the properties of reinforcing steel bars. *Construction and Building Materials* **2001,** *15* (8), 361-368.
38. Zhang, P.; Li, S. X.; Zhang, Z. F., General Relationship between Strength and Hardness. *Materials Science and Engineering: A* **2011,** *529*, 62-73.
39. Tekkaya, A. E.; Lange, K., An Improved Relationship between Vickers Hardness and Yield Stress for Cold Formed Materials and its Experimental Verification. *CIRP Annals - Manufacturing Technology* **2000,** *49* (1), 205-208.
40. Khaled, K. F., New Synthesized Guanidine Derivative as a Green Corrosion Inhibitor for Mild Steel in Acidic Solutions. *Int. J. Electrochemical Science* **2008,** *3*, 462-475.
41. Berduque, A.; Dou, Z.; Xu, R., Electrochemical Studies for Aluminium Electrolytic Capacitor Applications: Corrosion Analysis of Aluminium in Ethylene Glycol-Based Electrolytes. In *CARTS - Europe Virtual Conference*, Electronic Components Assoc. Inc.: Arlington, Virginia, USA, 2009; pp 1-10.
42. Bagotsky, V. S., *Fundamentals of Electrochemistry*. John Wiley & Sons, Inc.: Hoboken, New Jersey USA, 2006; pp.82.
43. Cynthia G. Zoski, *Handbook of Electrochemistry*. First ed.; Elsevier B.V.: Amsterdam, The Netherlands, 2007; pp.16.
44. Pistofidis, N.; Vourlias, G.; Konidaris, S.; Pavlidou, E.; Stergiou, A.; Stergioudis, G., Microstructure of zinc hot-dip galvanized coatings used for corrosion protection. *Materials Letters* **2006,** *60* (6), 786-789.
45. Fu, X.; Chung, D. D. L., Effect of corrosion on the bond between concrete and steel rebar. *Cement and Concrete Research* **1997,** *27* (12), 1811-1815.
46. Cheng, A.; Huang, R.; Wu, J. K.; Chen, C. H., Effect of rebar coating on corrosion resistance and bond strength of reinforced concrete. *Construction and Building Materials* **2005,** *19* (5), 404-412.

APPENDIX-A

Steel rebar test report

Bill To:
STEEL AND PIPE SUPPLY
P.O. BOX 1688
MANHATTAN KS
66502 US

Ship To: 14
STEEL AND PIPE SUPPLY CO
TULSA WAREHOUSE
1050 FORT GIBSON RD
CATOOSA OK
74015 US

Order Date:11/18/2010
PO No:4500150132
Mill Order No:3812776
Load No:1341415
Manifest No:2039174

CERTIFIED MATERIAL TEST REPORT
GERDAU AMERISTEEL
Midlothian Mill
300 Ward Road
Midlothian, TX 76065
(972)775-8241

SIZE	GRADE	LENGTH	PRODUCT
# 4 REBAR/13 MM / 13 MM	40/280	20 FT / 6.096 M	REBAR

SPECIFICATIONS
ASTM A615/A615M-09

HEAT NO: 11905560

CHEMICAL ANALYSIS

C	Mn	P	S	Si	Cu	Ni	Cr	Mo	Sn	V	Al	Nb
.32	.84	.019	.015	.24	.28	.08	.31	.029	.011	.003	.004	.000

PHYSICAL PROPERTIES

Yield Strength		Tensile Strength		Specimen Area		Elongation		Bend Test	ROA
KSI	MPa	KSI	MPa	Sq In	Sq cm	%	Gage Length	Dia. Result	%
60.5	417.1	90.4	623.3	0.192	1.24	18.3	8 In 200 mm	3.5 PASS	

APPENDIX-B

Tensile strength to hardness conversion chart

TENSILE STRENGTH TO HARDNESS CONVERSION CHART						
Brinell		Vickers or Firth Hardness No.	Rockwell		Scleroscope No.	Approximate Tensile Strength 1000 psi
Dia. (mm): 3000-kg Load 10-mm Ball	Hardness No.		C 150-kgLoad 120 DiamondCone	B 100-kg Load 1/16" dia. Ball		
2.05	898					440
2.10	857					420
2.15	817					401
2.20	780	1150	70		106	384
2.25	745	1050	68		100	368
2.30	712	960	66		95	352
2.35	682	885	64		91	337
2.40	653	820	62		87	324
2.45	627	765	60		84	311
2.50	601	717	58		81	298
2.55	578	675	57		78	287
2.60	555	633	55	120	75	276
2.65	534	598	53	119	72	266
2.70	514	567	52	119	70	256
2.75	495	540	50	117	67	247
2.80	477	515	49	117	65	238

2.85	461	494	47	116	63	229
2.90	444	472	46	115	61	220
2.95	429	454	45	115	59	212
3.00	415	437	44	114	57	204
3.05	401	420	42	113	55	196
3.10	388	404	41	112	54	189
3.15	375	389	40	112	52	182
3.20	363	375	38	110	51	176
3.25	352	363	37	110	49	170
3.35	331	339	35	109	46	160
3.40	321	327	34	108	45	155
3.45	311	316	33	108	44	150
3.50	302	305	32	107	43	146
3.55	293	296	31	106	42	142
3.60	285	287	30	105	40	138
3.65	277	279	29	104	39	134
3.70	269	270	28	104	38	131
3.75	262	263	26	103	37	128
3.80	255	256	25	102	37	125
3.85	248	248	24	102	36	122
3.90	241	241	23	100	35	119
3.95	235	235	22	99	34	116
4.00	229	229	21	98	33	113
4.05	223	223	20	97	32	110
4.10	217	217	18	96	31	107
4.15	212	212	17	96	31	104
4.20	207	207	16	95	30	101
4.25	202	202	15	94	30	99
4.30	197	197	13	93	29	97
4.35	192	192	12	92	28	95
4.40	187	187	10	91	28	93
4.45	183	183	9	90	27	91
4.50	179	179	8	89	27	89
4.55	174	174	7	88	26	87

4.60	170	170	6	87	26	85
4.65	166	166	4	86	25	83
4.70	163	163	3	85	25	82
4.75	159	159	2	84	24	80
4.80	156	156	1	83	24	78
4.85	153	153		82	23	76
4.90	149	149		81	23	75
4.95	146	146		80	22	74
5.00	143	143		79	22	72
5.05	140	140		78	21	71
5.10	137	137		77	21	70
5.15	134	134		76	21	68
5.20	131	131		74	20	66
5.25	128	128		73		65
5.30	126	126		72		64
5.35	124	124		71		63
5.40	121	121		70		62
5.05	140	140		78	21	71
5.10	137	137		77	21	70
5.15	134	134		76	21	68
5.20	131	131		74	20	66
5.25	128	128		73		65
5.30	126	126		72		64
5.35	124	124		71		63
5.40	121	121		70		62

VITA

HYMAN JAFAR JAAF

Candidate for the Degree of

Master of Science

Thesis: THE EFFECT OF COLD GALVANIZING ZINC COATING AS A CATHODIC PROTECTION ON CORROSION RATE AND BOND STRENGTH OF REINFORCED CONCRETE

Major Field: Chemical engineering

Biographical:

Education:

Completed the requirements for the Master of Science in Chemical Engineering at Oklahoma State University, Stillwater, Oklahoma in December 2012.

Completed the requirements for the Bachelor of Engineering in Chemical Engineering Department in University of Technology, Baghdad, Iraq in 1993.

Experience:

Work as an engineer in College of Engineering, Al-Mustansiriya University, in Baghdad, Iraq. Responsibilities include technical management of sanitary laboratory, technical supervising the experimental work of undergraduate students in the chemical laboratory, technical supervising the application work of undergraduate students in the computer laboratory, technical supervising the experimental work of undergraduate students in the sanitary laboratory, and conducting water quality tests for raw water, drinking water, and sewage water.

Professional Memberships:

Member in Iraqi Engineers Union.